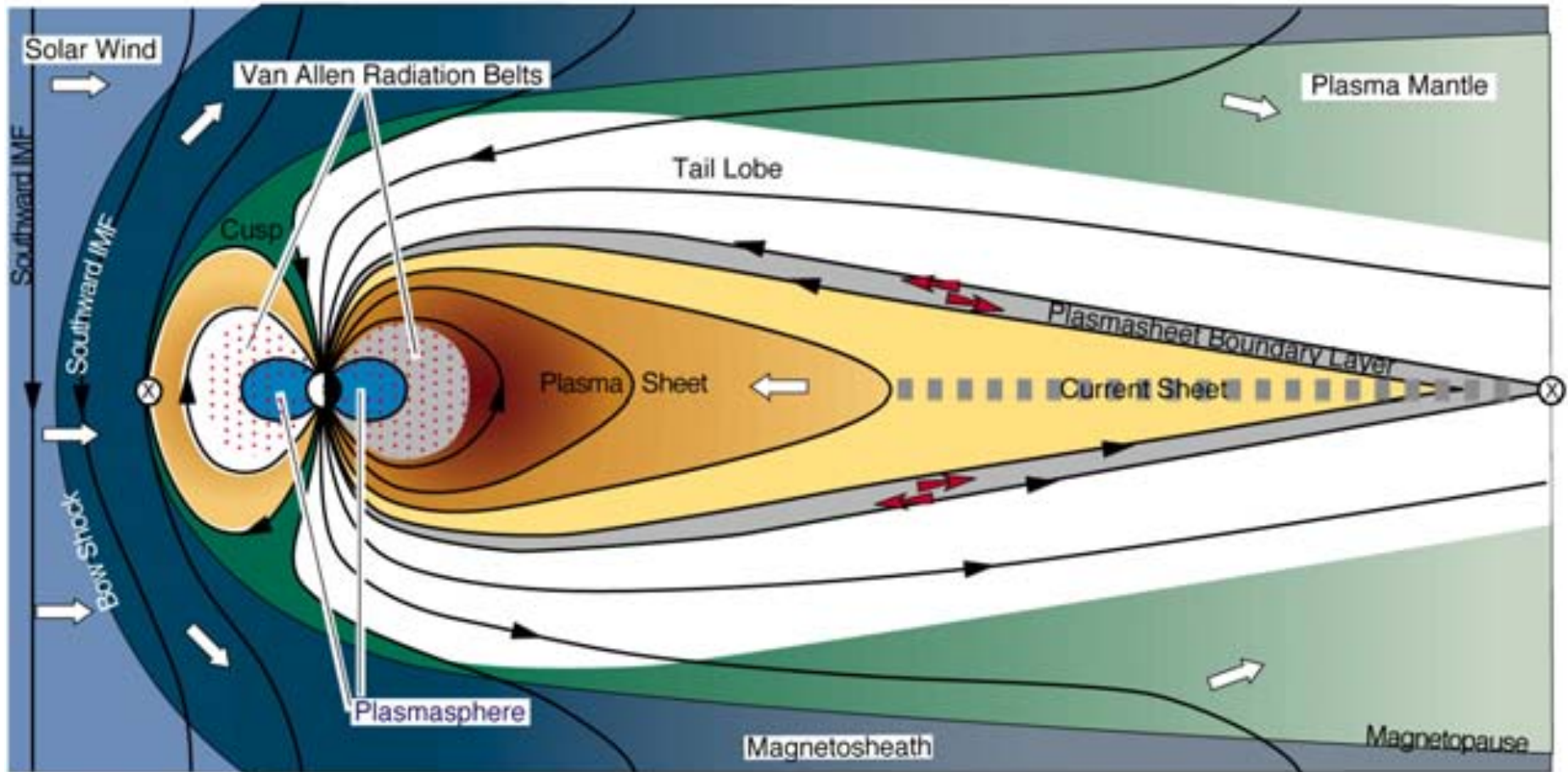


# Solar Wind Magnetosphere Coupling



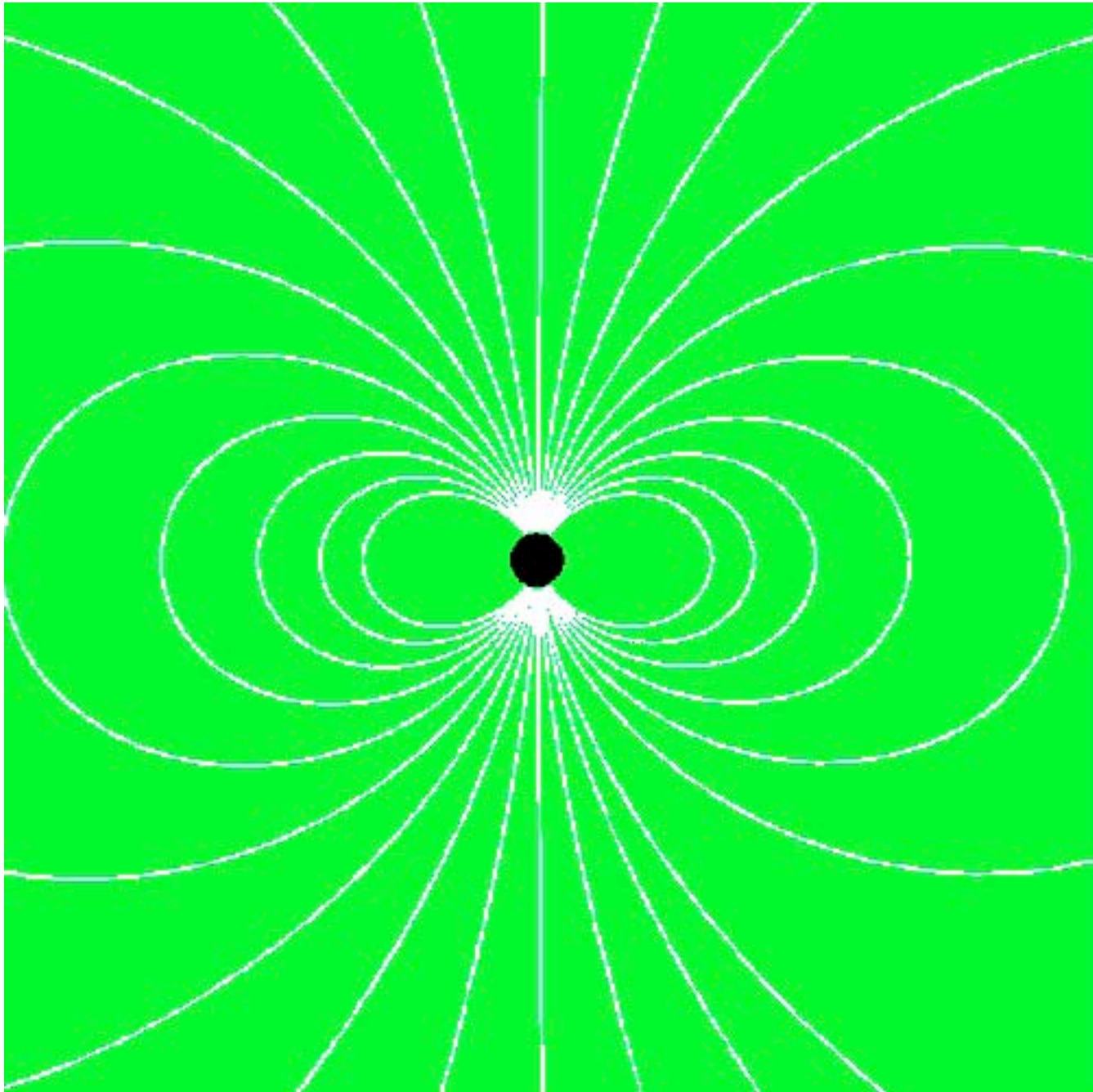
Frank Toffoletto, Rice University

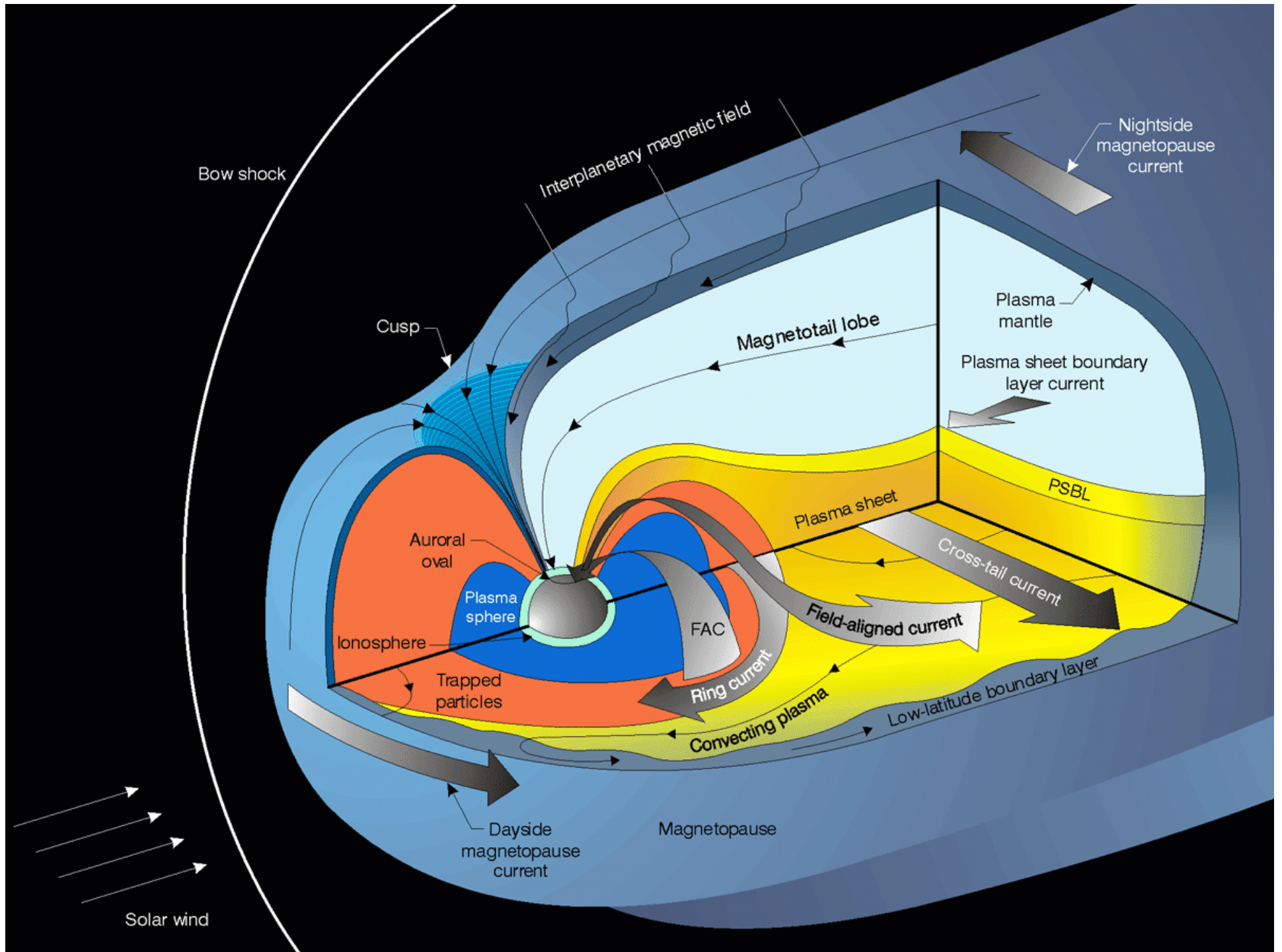
Figure courtesy T. W. Hill

thanks to R. W. Spiro, R. A. Wolf and T. W. Hill, Rice U.

# Outline

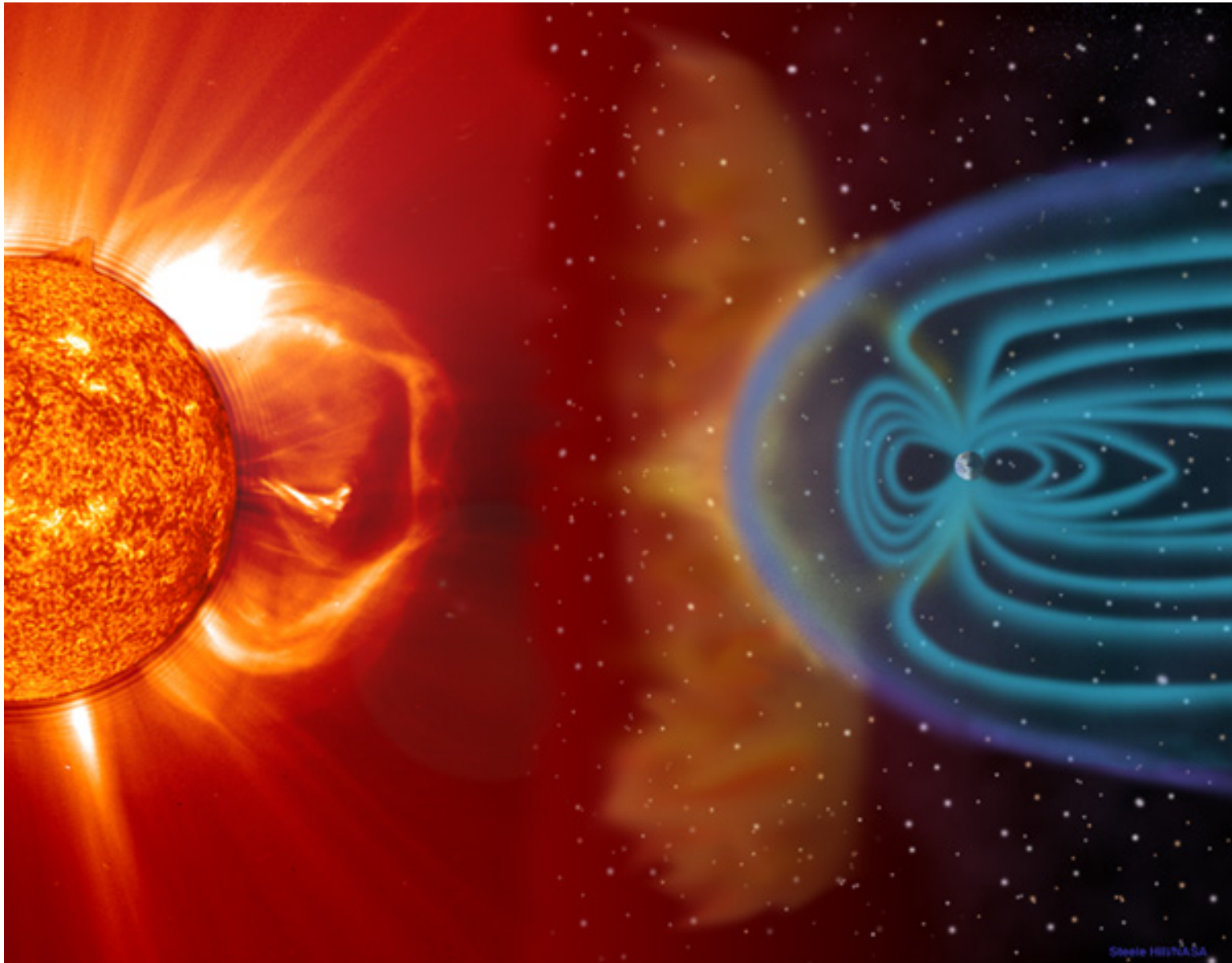
- Introduction
- Properties of the Solar Wind Near Earth
- The Magnetosheath
- The Magnetopause
- Basic Physical Processes that control Solar Wind Magnetosphere Coupling
  - Open and Closed Magnetosphere Processes
  - Electrodynamic coupling
  - Mass, Momentum and Energy coupling
  - The role of the ionosphere
- Global MHD codes at CCMC
- Current Status and Summary





# Introduction

- By virtue of our proximity, the Earth's magnetosphere is the most studied and best understood magnetosphere
  - However, the system is rather complex in its structure and behavior and there are still some basic unresolved questions
  - Today's lecture will focus on describing the coupling to the major driver of the magnetosphere
    - The solar wind, and the ionosphere

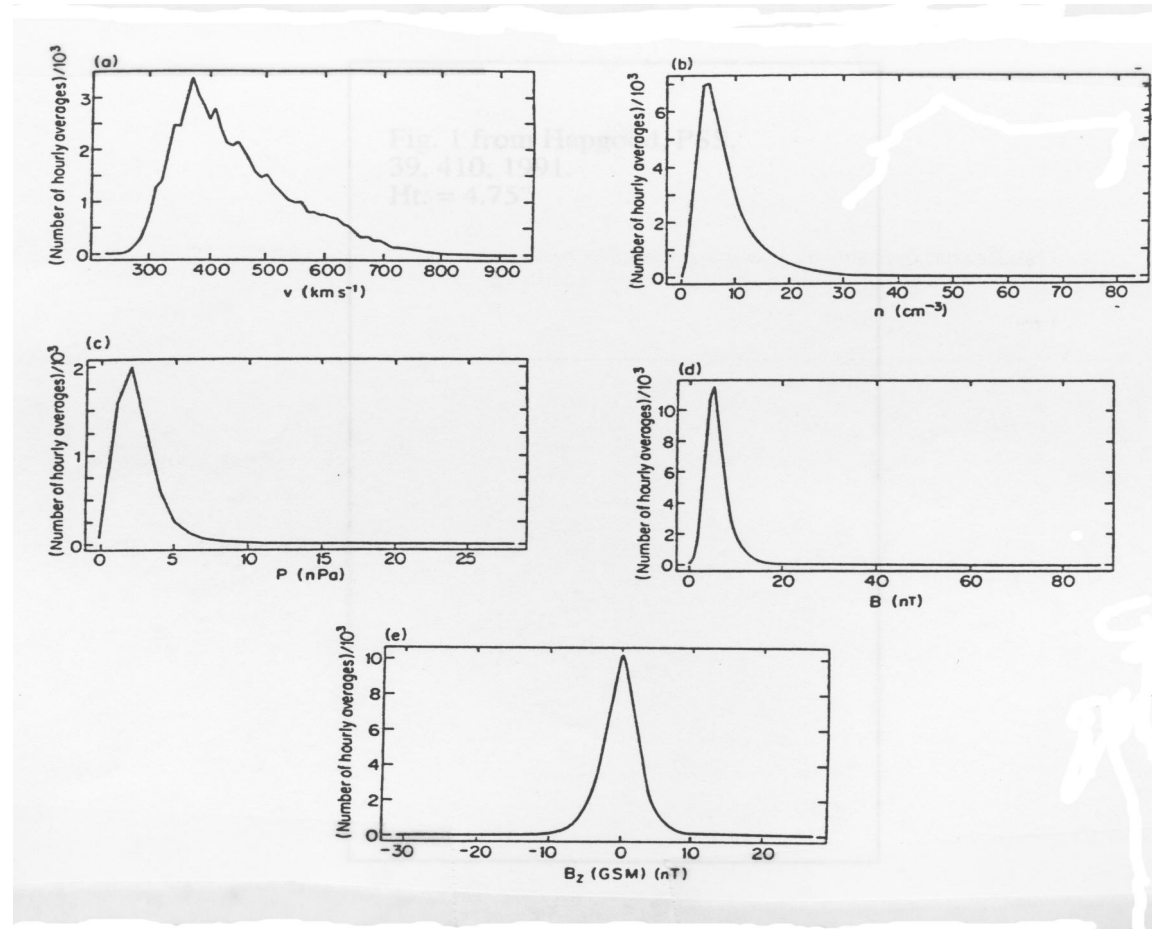


Steele Hill/NASA

Figure courtesy NASA

# The Solar Wind Near the Earth

# Solar-Wind Properties Observed Near Earth



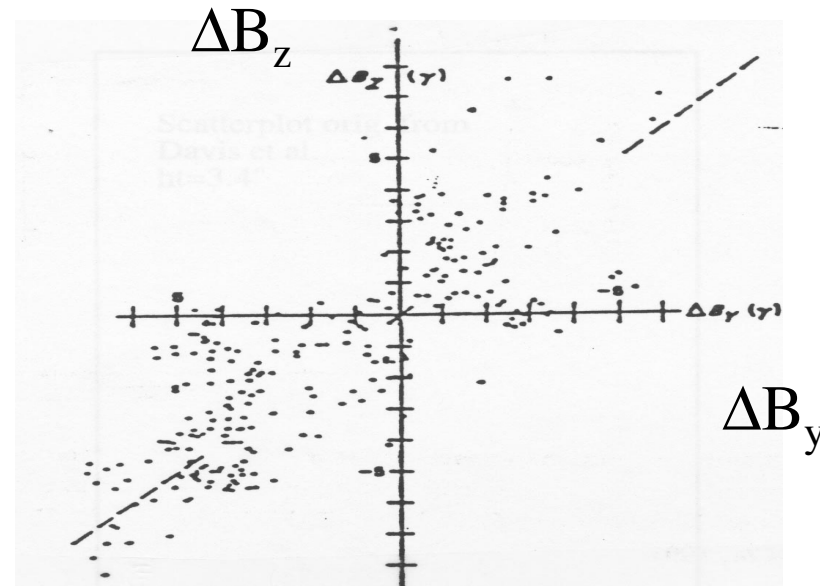
- Solar wind parameters observed by many spacecraft over period 1963-86. From Hapgood et al. (Planet. Space Sci., 39, 410, 1991).

# Solar Wind Observed Near Earth

Parameter	Mean	$\sigma$	Median	5-95% range limit	Observed min and max values
Number Density ( $\text{cm}^{-3}$ )	8.7	6.6	6.9	3-20	0.1-83
Velocity (km/s)	468	116	442	30-270	250-2000
Ram Pressure $\rho v^2$ (nPa)	7	5.2	5.5	0.01-14.5	0.05-28
Magnetic Field (nT)	6.2	2.9	5.6	2.2-9.9	0-85
Ion Temp. ( $10^5\text{K}$ )	1.2	0.9	1.0	0.1-3	0.1-3
Electron Temp. ( $10^5\text{K}$ )	1.4	0.4	1.3	0.9-2	1-2

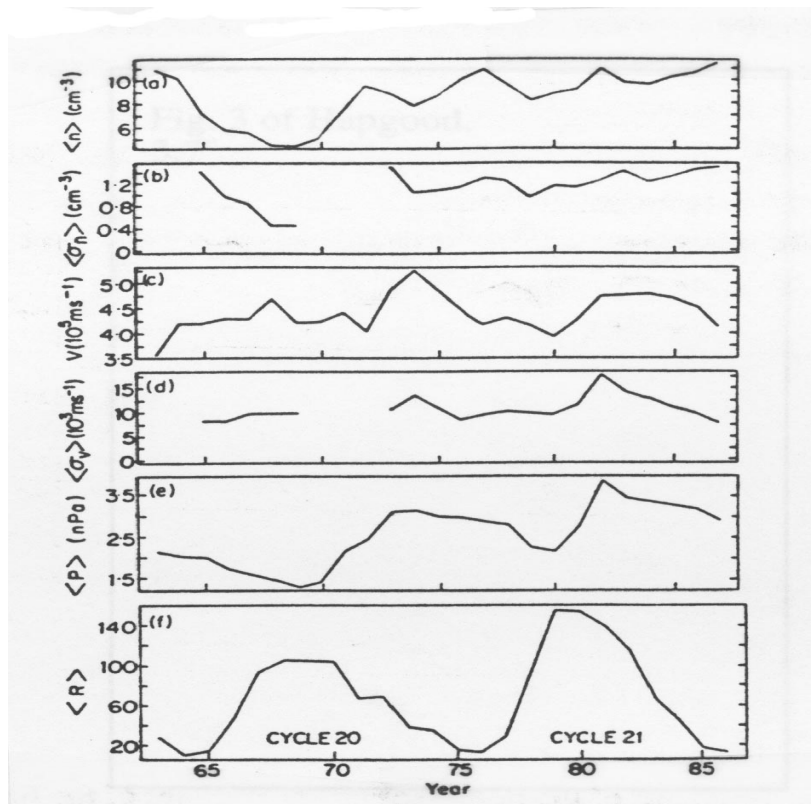
From Feldman et al. (Solar Output and its Variations, Colorado Assoc. Univ. Press, 1977)

# Solar Wind Observed Near Earth



- Observed near Earth, the interplanetary magnetic field tends to make  $\sim 45^\circ$  or  $\sim 225^\circ$  angle with Sun-Earth direction.
  - Parker spiral.
- The north-south component of the IMF averages near zero and fluctuates on short time scales

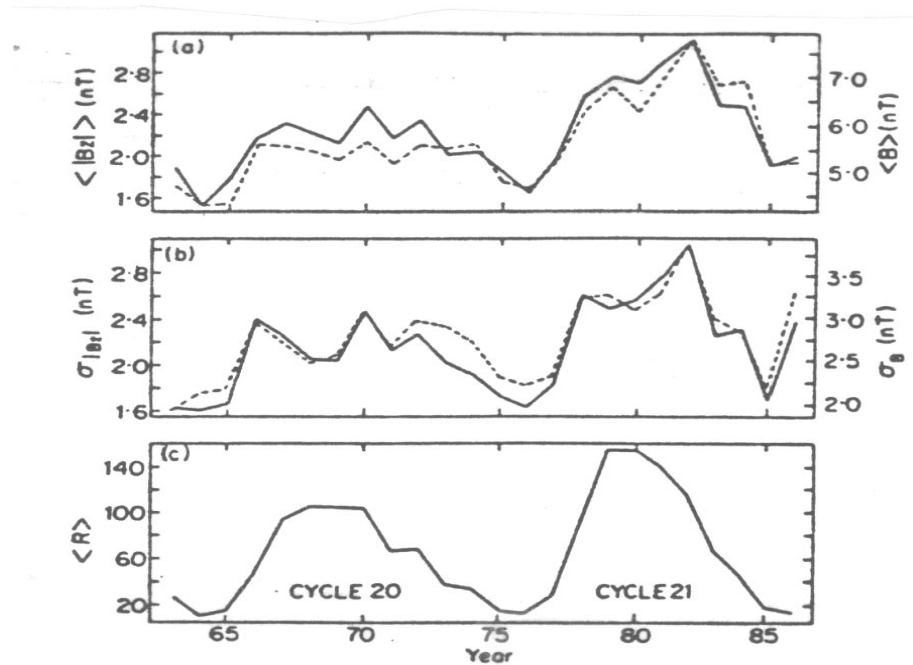
# Solar-Cycle Variation of Solar Wind Near Earth



From Hapgood et al.  
(1991)

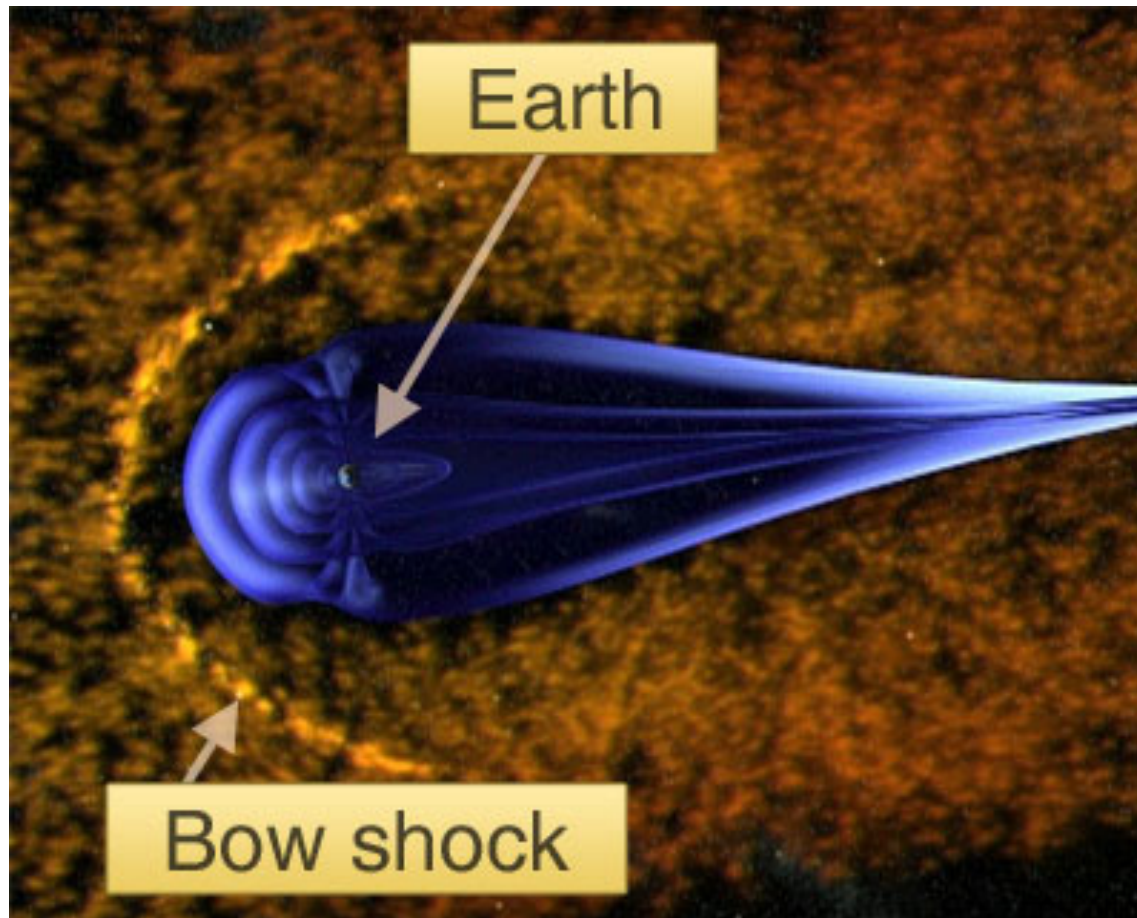
- Average velocity highest in declining phase of solar cycle.
- Successive solar cycles represent different polarities of Sun's magnetic field.
- Magnetic-field reversal occurs near solar maximum.

# Solar-Cycle Variation of Solar Wind Near Earth



- Plot shows average absolute value of north-south IMF component.
- Highest near solar maximum.

# The Magnetosheath



ESA

- The energy of the solar wind has 3 components:
  - Thermal
  - Magnetic
  - Flow
- Which has the largest energy density?

# Energy Densities in Solar Wind Near Earth

$$\left(\frac{1}{2}\rho v^2\right)_{sw} \approx \frac{1}{2}(1.67 \times 10^{-27} \text{ kg})(6 \text{ cm}^{-3})(370 \text{ km/s})^2 \approx 7 \times 10^{-10} \text{ J/m}^3$$

$$\left\langle \frac{B^2}{2\mu_0} \right\rangle \approx \frac{(6nT)^2}{8\pi \times 10^{-7}} \approx 1.4 \times 10^{-11} \text{ Jm}^{-3} \sim 0.02 \left(\frac{1}{2}\right) \rho v^2$$

$$\left\langle \frac{3}{2}nk(T_e + T_i) \right\rangle \approx \frac{3}{2}(6 \text{ cm}^{-3})(1.38 \times 10^{-23})(1.2 + 1.4)10^5 \sim 3 \times 10^{-11} \text{ J/m}^3$$

$$\rho v^2 \gg p \quad \text{or} \quad \frac{B^2}{2\mu_0}$$

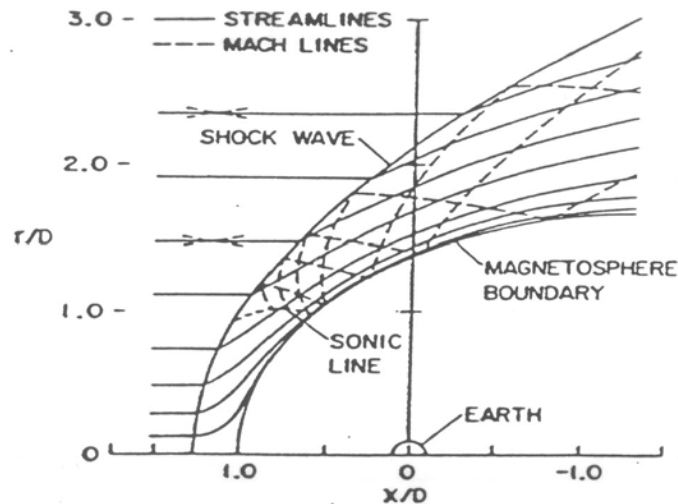
$$\langle M_A \rangle = \left\langle \frac{v}{\sqrt{\frac{B^2}{\mu_0 \rho}}} \right\rangle \sim 7 \quad \langle M_S \rangle = \left\langle \frac{v}{\sqrt{\frac{5p}{3\rho}}} \right\rangle \sim 8$$

- Flow controls the magnetic field, drags it along.
  - Magnetic field is essentially frozen to the plasma

# Magnetosheath– Gasdynamic Aspects

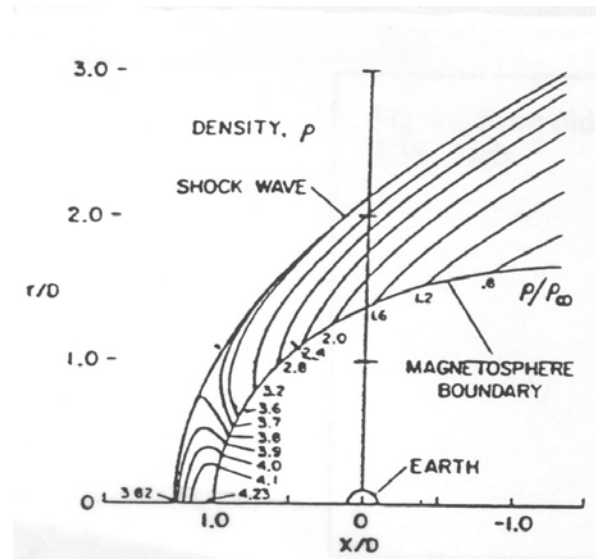
- The energy of the solar wind is dominated by the flow
- The theoretical way to deal with this is to treat the flow as gasdynamic and to neglect the magnetic field.
  - Back in the 1960' s, John Spreiter and colleagues converted an existing numerical code to describe the bow shock and magnetosheath. The code had been developed to treat the flow around missiles.
  - They assumed an axially symmetric shape for the magnetopause.
- Since the solar wind is supersonic, it forms a shock as it encounters the Earth' s magnetosphere and slows down
  - The collision mean free path of the solar wind is of the order of  $\sim 10^6 R_E$ , the thickness of the bow shock is of the order of the ion gyroradius ( $\sim 1000$  km)

# Streamlines and Mach Lines



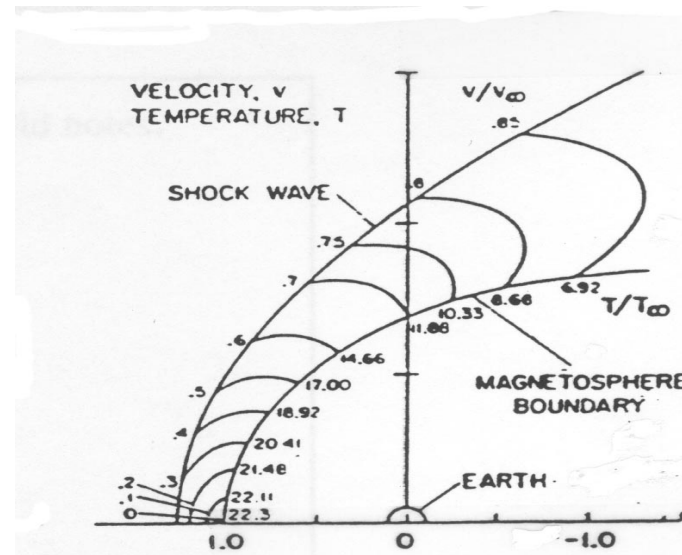
- This computation was for Mach number 8,  $\gamma = 5/3$ .
- The code computes the position of the shock self-consistently.
- Flow diverts around the obstacle, which is assumed impenetrable.
- The flow gets very slow right at the nose of the magnetosphere.
  - Flow accelerates away from there.
  - Flow becomes supersonic at the “sonic line.”

# Density Distribution



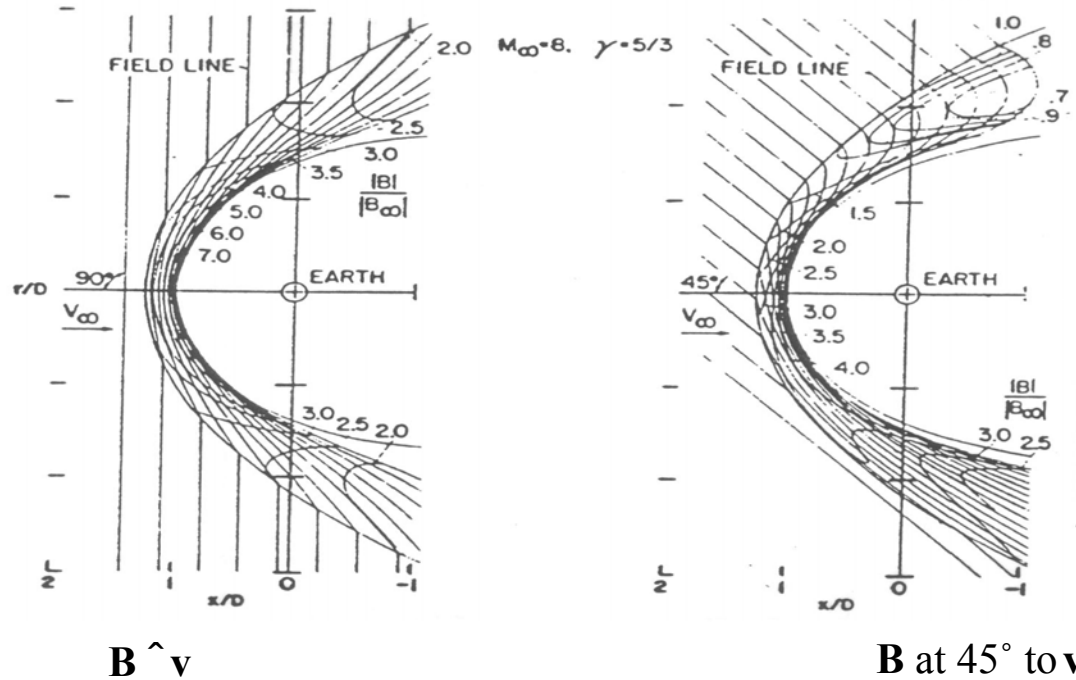
- Density:
  - For Mach number 8 and  $\gamma = 5/3$ , the model calculation indicates that the density jumps by a factor 3.82 across the shock.
  - Max density is at “subsolar point,” 4.23 times solar wind density.
  - Density gradually decreases away from subsolar point.

# Velocity and Temperature Distributions



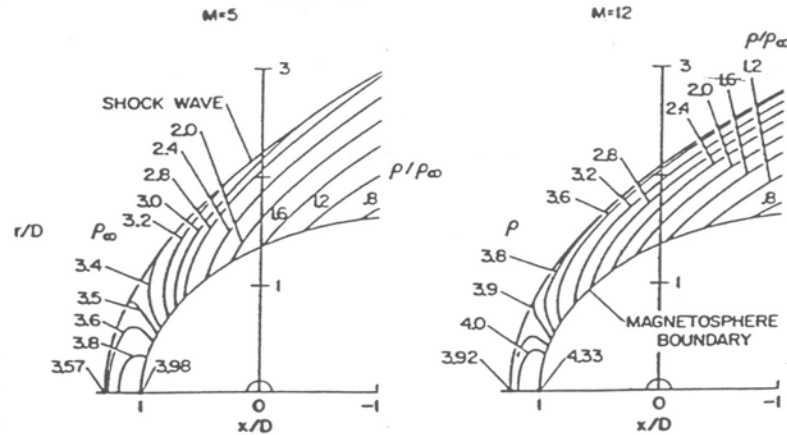
- Temperature decreases away from subsolar point
- Velocity increases away from that point.
- The contours for  $T$  and  $v$  are the same.

# Magnetic Field Distribution

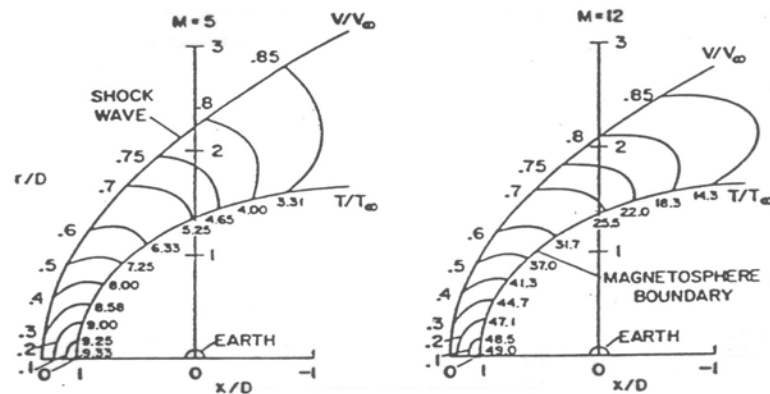


- Computed from assumption of frozen-in flux
- Note how magnetic field lines hang up on nose of magnetosphere
- B highest near subsolar point.
  - Zwan-Wolf effect
- In reality, the magnetosheath is very noisy

# Effects of Mach Number

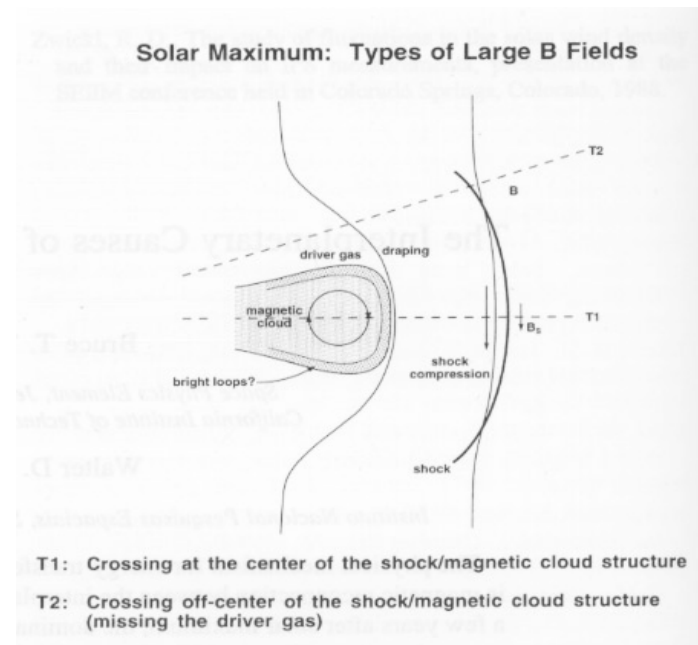


Effect of Mach number on density field for flow past the magnetosphere.  $\gamma = 5/3$ . From Spreiter et al. (1968), *ibid*.



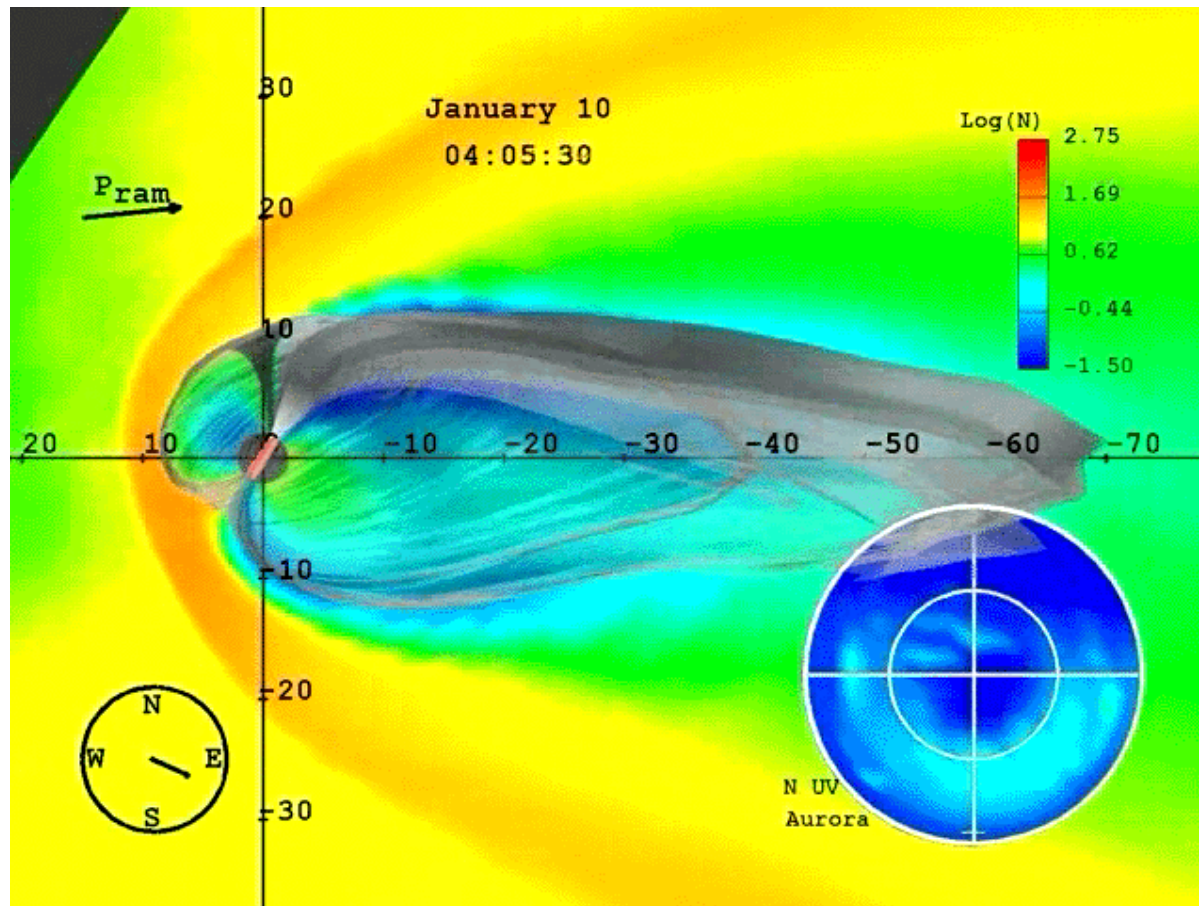
Effect of Mach number on velocity and temperature fields for flow past the magnetosphere, for  $\gamma = 5/3$ . From Spreiter et al. (1968), *ibid*.

# Magnetic Cloud Events



- Most very large magnetic storms on Earth are caused by magnetic clouds or “islands.”
  - Strong organized magnetic field
  - Long period of northward field and long period of southward field.
    - Southward field causes storm

# Magnetopause formation



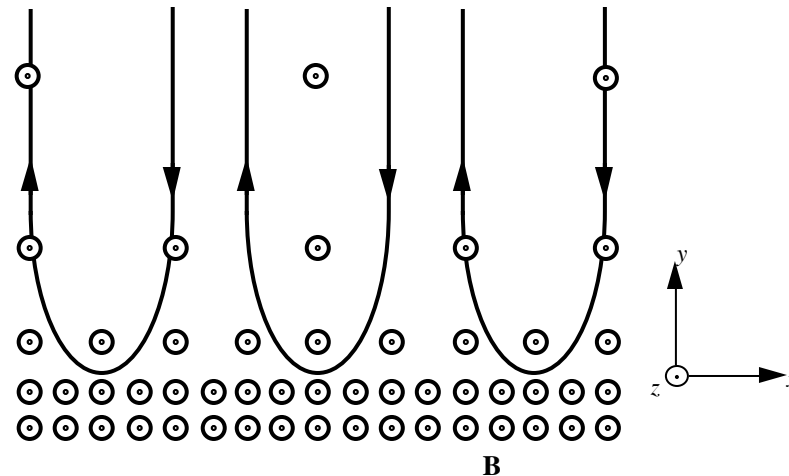
Snapshot from the LFM global magnetosphere code

# Definition of “Magnetopause”

- An observer would want to define it in terms of something that is easy to observe, like a sharp jump in ‘something’ .
- A theorist would want to define it in profound theoretical terms, such as the boundary between open and closed field lines.
  - However, that theorist’s definition doesn’t work - isn’t consistent with the established definition of the magnetosphere, which is the region dominated by Earth’s magnetic field.
  - Polar caps lie on open field lines, but at low altitudes they certainly lie in a region dominated by Earth’s field.
- We use an observational definition--a sharp change in the magnetic field.

# Solar-Wind/Magnetosphere Coupling— Basic Physical Processes

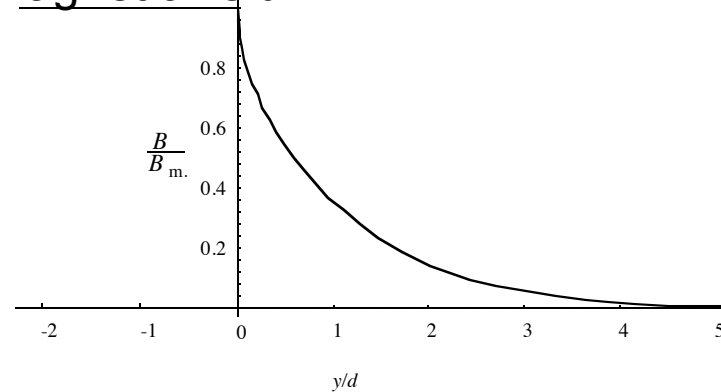
## Theories of an Ideal Magnetopause Chapman-Ferraro Magnetopause



- 1D picture of the magnetopause, assuming unmagnetized solar wind  $\mathbf{v} = -v_o \hat{\mathbf{e}}_x$
- Assume incident beam with density  $n_o$ ,
- Magnetic field assumed parallel to z.
- Assume zero electric field.

# Chapman-Ferraro-Type Magnetopause

- Solution for the magnetic field:



- The B-field scale length is related to the gyroradius inside the magnetosphere:

$$a_{cm} = \frac{mv_o}{qB_m} = \frac{d}{\sqrt{2}}$$

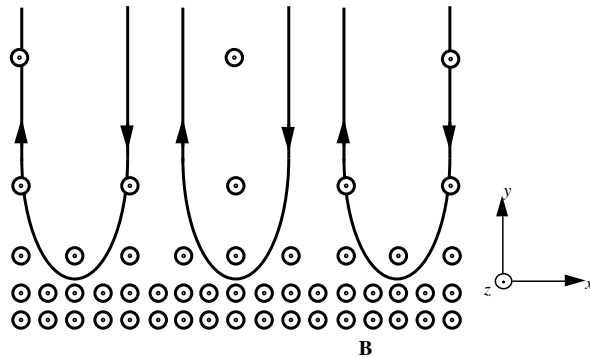
- The momentum/area/time that the particles impart to the magnetic boundary is

$$2n_o m v_o^2 = \frac{B_m^2}{2\mu_o}$$

– Intuitively reasonable

- **The most fundamental conclusion of Chapman and Ferraro was that a boundary would form between the solar wind and magnetosphere, and that the solar wind would basically not penetrate to the space near Earth.**

# Chapman-Ferraro-Type Magnetopause

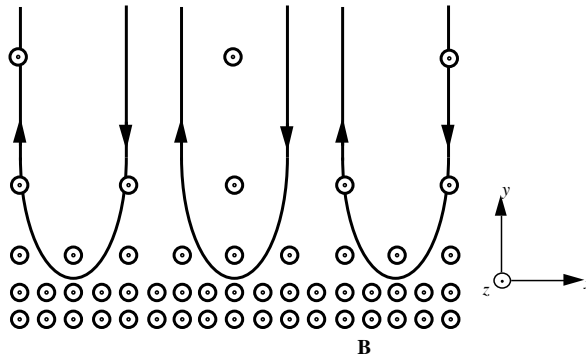


- One problem: charge imbalance:
  - Solar wind electrons presumably have the same density and flow velocity as the ions.
  - The electrons are much easier to turn around than the more massive ions
  - There is a negative charge layer above the positive charge layer
  - Order-of-magnitude estimate:

$$\text{Surface charge density} = \sigma_c \sim n_o q d$$

$$\Delta V \sim \frac{\sigma_c d}{\epsilon_o} \sim \frac{m_i}{2\mu_o \epsilon_o q} \sim \frac{m_i c^2}{2q} \sim 500 \times 10^6 V$$

# Chapman-Ferraro-Type Magnetopause



- Such a large potential drop can't be driven by particles  $\sim 1$  keV
- Chapman and Ferraro realized this, and they enforced quasi-neutrality and calculated a self-consistent electric field.
  - They calculated a potential drop  $\sim mv_o^2/2$
- Parker later pointed out that the magnetopause field lines connect to the conducting ionosphere.
  - If the charge density were maintained for a substantial time, then charges would flow up to and from the ionosphere, to eliminate the charge imbalance.

# Models with a Self-Consistently Computed Magnetopause

- The first models with a self-consistently computed magnetopause were developed in the early 1960' s.
- Assume

$$\mathbf{B}_o = 0$$

where “o” means outside the magnetopause. Since,  $\nabla \cdot \vec{B} = 0$  we require

$$\mathbf{B}_i \cdot \hat{\mathbf{n}} = 0$$

The total pressure in the magnetosheath just outside the magnetopause is estimated from the formula

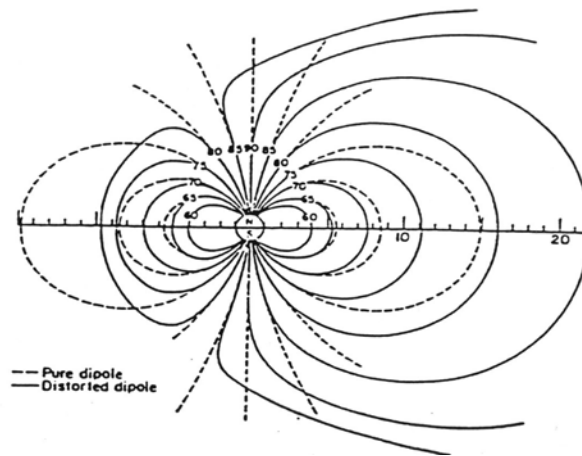
$$p_o = k\rho_{sw}(\hat{\mathbf{n}} \cdot \mathbf{v}_{sw})^2$$

$k=2$  corresponds to the Chapman-Ferraro model.  $k=1$  corresponds to particles sticking to the boundary.  $k=0.884$  corresponds to the gasdynamic model with  $\gamma=5/3$ ,  $M=8$ .

- The field just inside the magnetopause satisfies the pressure balance relation

$$\frac{|\hat{\mathbf{n}} \times \mathbf{B}_i|^2}{2\mu_o} = k\rho_{sw}(\hat{\mathbf{n}} \cdot \mathbf{v}_{sw})^2$$

# Models with a Self-Consistently Computed Magnetopause



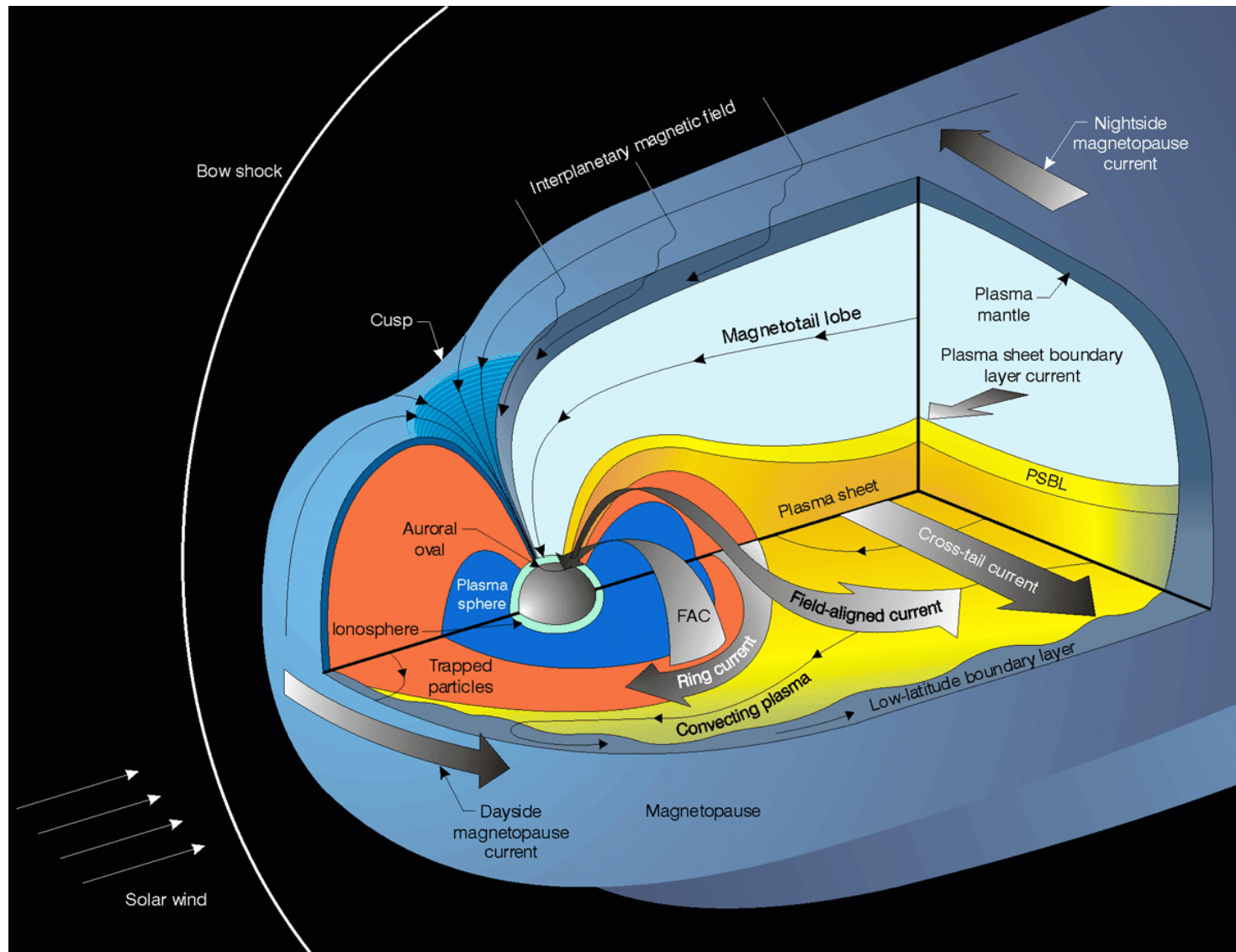
Mead (1964) model

- This model has a self-consistently computed magnetopause
  - No magnetotail (wasn't discovered until 1965)
  - Assumed  $\nabla \times \vec{B} = 0$  inside the magnetopause.

# Question

- In what direction is the magnetic field associated with the Chapman Ferraro currents?

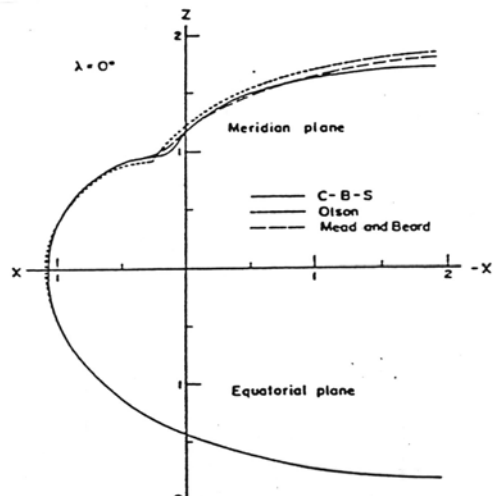
# Magnetospheric Current Systems



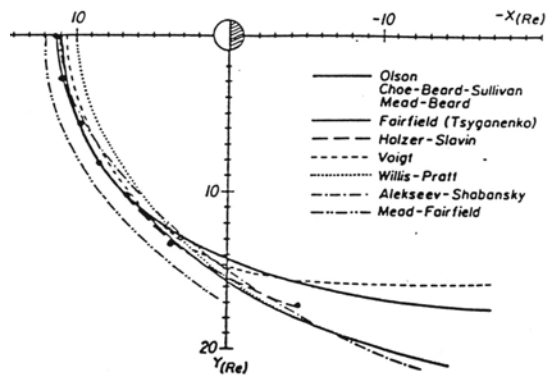
# Early Self-Consistently Computed Magnetopauses

3 versions of Choe/Beard/Sullivan model in noon-midnight plane.

[Q: Why is there an indentation?]



PROJECTION OF MAGNETOPAUSE BOUNDARIES ON EQUATORIAL PLANE



Model equatorial cross section

# Dependence of Standoff Distance on Solar-Wind Parameters

- Define

$$B_i^{subsolar} = 2 f B_{dipole}^{subsolar}$$

- The real magnetopause is between these two extremes.
- The results of the problem suggest that

$$1.0 \leq f \leq 1.5$$

- The pressure-balance relation becomes

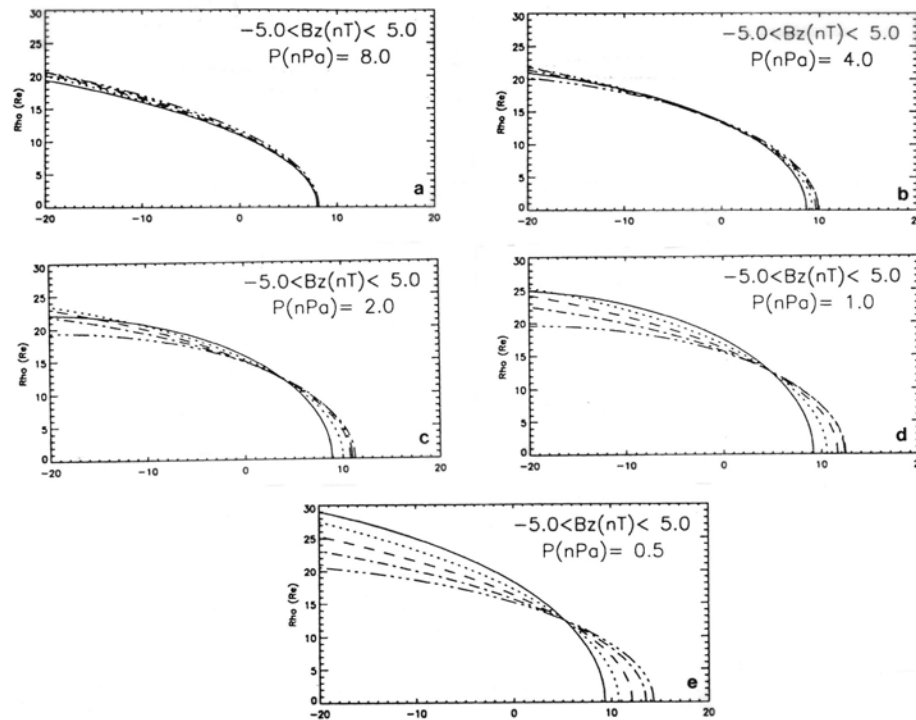
$$k \rho_{sw} v_{sw}^2 = \frac{1}{2\mu_o} \left[ 2 f B_o \left( \frac{R_E}{r_{so}} \right)^3 \right]^2$$

- Solving for  $r_{so}$  gives

$$r_{so} = R_E \left( \frac{2 f^2 B_o^2}{k \mu_o \rho_{sw} v_{sw}^2} \right)^{1/6} = \frac{11.43 R_E}{\left( \rho_{sw} v_{sw}^2 \right)_{nPa}^{1/6}} \left( \frac{f}{1.16} \right)^{1/3} \left( \frac{0.885}{k} \right)^{1/6}$$

The best-estimate value for  $f$  is about 1.16 . A nominal solar wind (5  $\text{cm}^{-3}$ , 400 km/s) corresponds to  $\rho_{sw} v_{sw}^2 = 1.34 \text{ nPa}$ , which corresponds to  $r_{so} = 10.9$

# Empirical Magnetopause Shapes



Average observed shape of magnetopause. Solid curve is -5 nT, dotted curve -2.5nT, dashed curve 0, dash-dot 2.5 nT, dash-dot-dot 5.0 nT. Adapted from Roelof and Sibeck (JGR, 99, 8787, 1994)

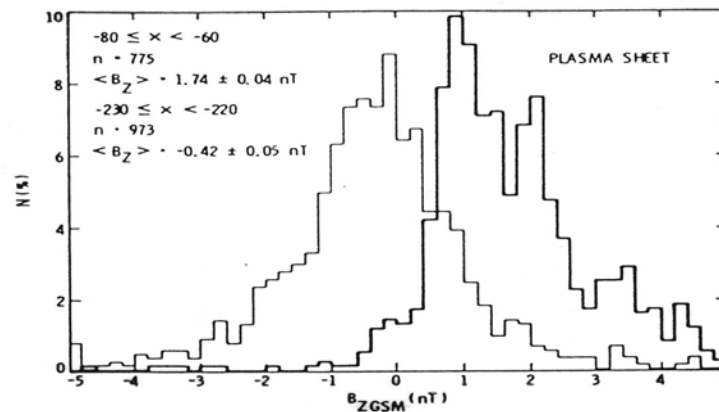
- Note
  - Southward IMF moves magnetopause closer to Earth, strengthens tail lobes.
- Magnetopause position doesn't vary over a wide range (1/6 th power)
  - Subsolar standoff distance is nearly always between  $6.6 R_E$  and  $14 R_E$ .



# Decline of $B_z$ Downtail

- For  $x > -20$ ,
  - $B_z$  is nearly always positive on the flanks of the tail, occasionally negative near local midnight
  - The  $B_z$  distributions are much broader (indicating more variability)
    - Suggests both occasional x-lines earthward of -20.
    - Consistent with dipolarization of field in expansion phase.
- For  $-45 < x < -20$ ,
  - $|B_z|$  smaller.
  - Sector doesn't matter much.

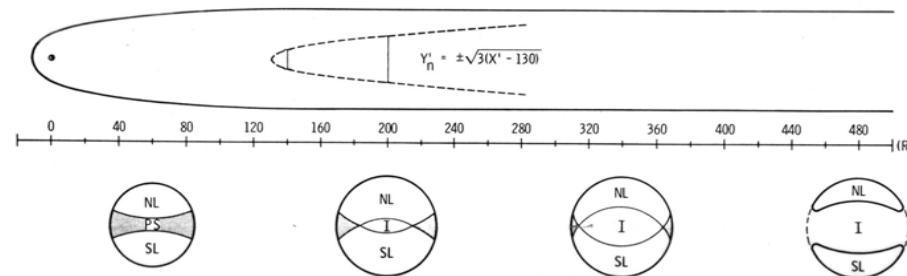
# $B_z$ Further Downtail



Histograms of z component of B in plasma sheet, from ISEE-3. From Siscoe et al.(1984).

- 60-80  $R_E$  behind Earth,  $B_z$  is still usually positive.
- 225  $R_E$  behind Earth,  $B_z$  is negative more than half the time.

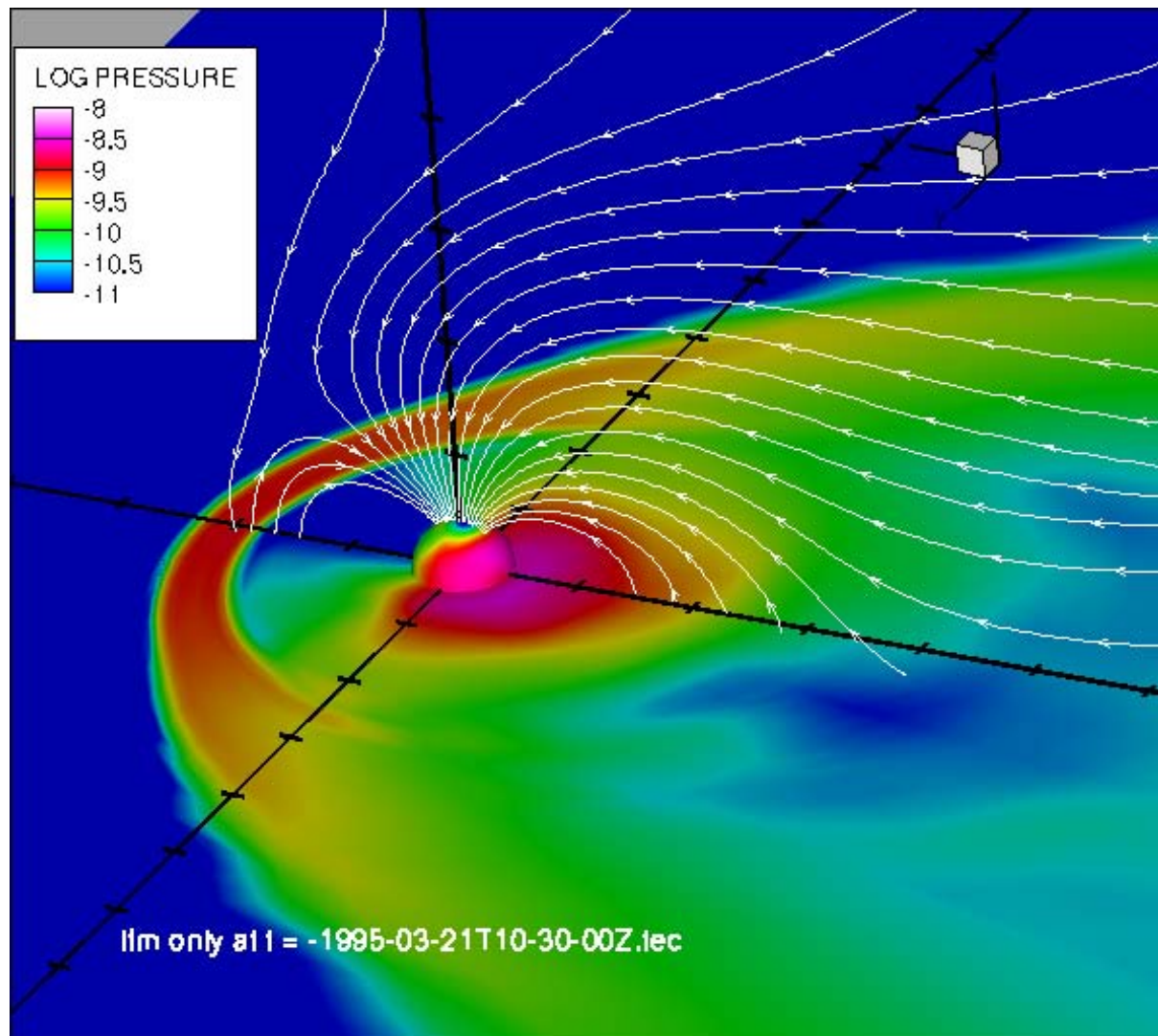
# Where Does Average $B_z$ Turn Negative?



Location of separatrix between interplanetary field lines and closed field lines, from Slavin et al. (1985).

- Neutral line of average  $B_z$ :
  - $\sim 130 R_E$  near local midnight
  - $\sim 300 R_E$  on the flanks
- The “wake”, which consists of field lines that are connected to the interplanetary medium on both “ends”, becomes a larger and larger part of the tail as you go downstream.

# Coupling processes



# Basic Magnetospheric Convection

- Solar Wind Magnetosphere Coupling produces a system of plasma convection
  - Plasma in to the high latitude region connected to the outermost layers of the magnetosphere flow anti-sunward
  - Plasma in to the low latitude connected to the inner magnetosphere generally flow sunward
  - The presence of such convection suggest some form of drag or frictional force acting across the magnetopause

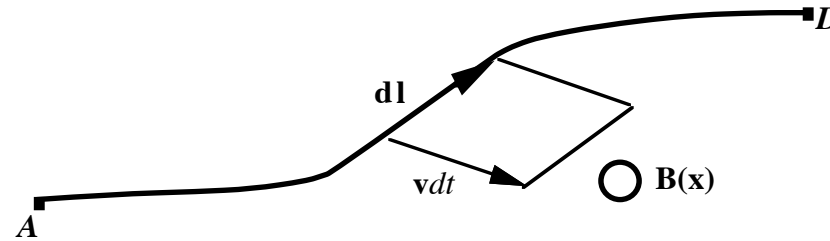
# The Real Magnetopause apparently Isn't Ideal

- An ideal magnetopause – Chapman-Ferraro or tangential-discontinuity–has no mass flow across the boundary, no energy flux, no drag force.
- Some particles are observed in the magnetosphere that are clearly from the solar wind ( $\text{He}^{++}$ , for example).
- The long tail suggests that there is a substantial drag force.
- A southward turning of the interplanetary magnetic field (IMF) causes increased energy dissipation in the ionosphere
  - Clearly suggests that energy flows across the magnetopause into the magnetosphere.
- Therefore, we need to consider processes that transport particles, energy, or drag force across the magnetopause.

# Transfer Processes at a Closed Magnetopause

- We will consider various closed-model transfer processes and try to estimate how efficient each is.
  - The crucial thing that we must explain is the rate of magnetospheric convection, the rate of circulation of plasma around the magnetosphere.
    - This turns out to be key--the observed rate of convection turns out to be harder to explain quantitatively than the observed rate of transfer of mass, momentum, and energy.
- How does one quantitatively characterize the rate of plasma circulation?
  - In ideal MHD, there is a simple answer: a voltage.

## Potential Drop as a Measure of Convection



- How many field lines cross  $AD$  per unit time, assuming the perfect-conductivity relation

$$\mathbf{E} + \mathbf{v} \times \mathbf{B} = 0$$

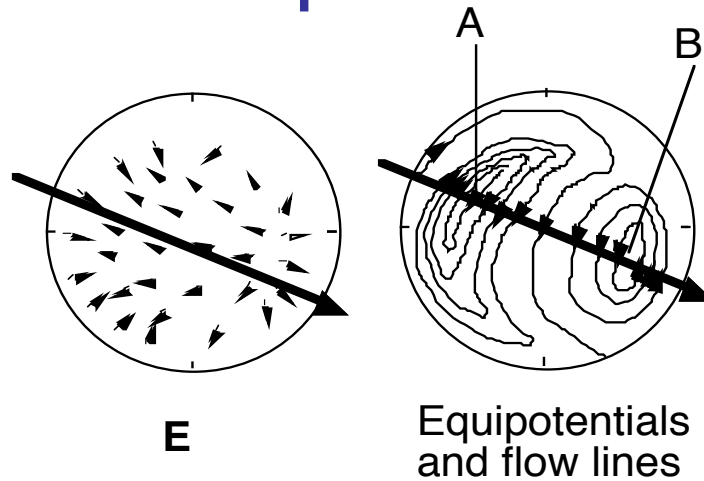
Consider field lines to move with the fluid elements that are locked to them.

$$\frac{d\Phi_M}{dt} = \frac{\int (\mathbf{v} dt) \times \mathbf{dl} \cdot \mathbf{B}}{dt} = - \int_A^D \mathbf{dl} \cdot \mathbf{v} \times \mathbf{B} = \int_A^D \mathbf{dl} \cdot \mathbf{E}$$

$$\frac{d\Phi_M}{dt} = - \int_A^D \mathbf{dl} \cdot \nabla \Phi = \Phi_A - \Phi_D$$

- Thus the number of magnetic flux tubes crossing  $AD$  per unit time is the potential difference between  $A$  and  $D$ .

# Polar-Cap Potential Drop

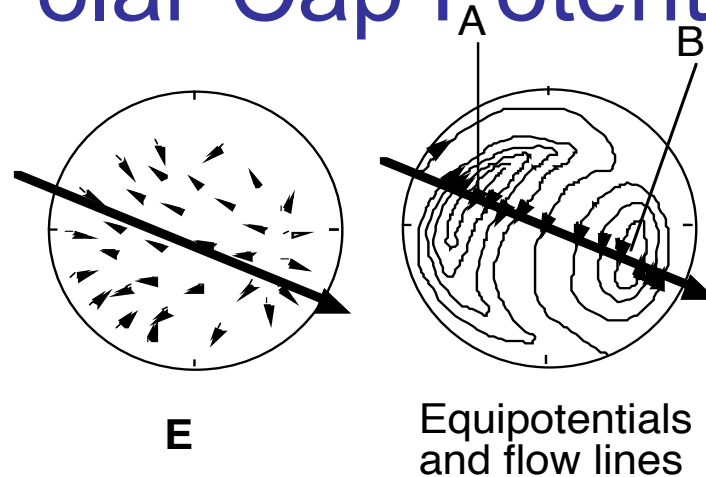


- The potential drop across the high-latitude ionosphere can be measured by a polar-orbiting spacecraft.

$$\Phi_{pcp} = \int_A^B \mathbf{E} \cdot d\mathbf{l}$$

- The polar cap potential drop  $\Phi_{pcp}$  is measured routinely by satellites traversing the high-latitude ionosphere.

# Polar-Cap Potential Drop

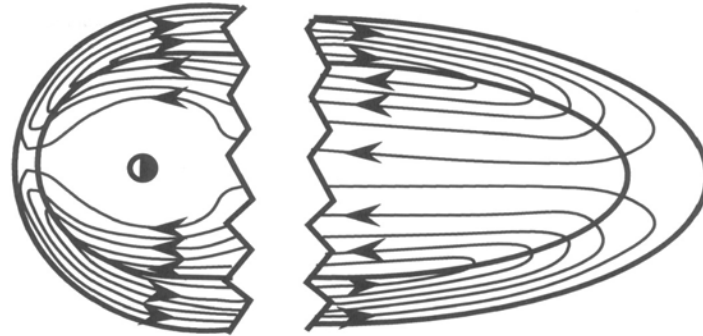


- Technical Problem: Satellite track doesn't usually cross either the max potential point *A* or the minimum potential point *B*.
  - Difference between max and min potential on satellite track is a lower limit on  $F_{pcp}$ .
  - Use only spacecraft in dawn-dusk orbit and estimate correction.
  - DMSP ion drift meter makes routine measurements of velocity perpendicular to the spacecraft track.
- Observed values:

$$20 \text{ kV} \leq \Phi_{pcp} \leq 250 \text{ kV}$$

$$\langle \Phi_{pcp} \rangle \approx 50 \text{ kV}$$

# Polar-Cap Potential Drop Driven by Viscous Interaction



(adapted from Hill, 1983)

- Originally suggested by Axford and Hines (1961).
- Assume that the field lines are approximately equipotentials.
- If the average observed polar cap potential (50 keV)

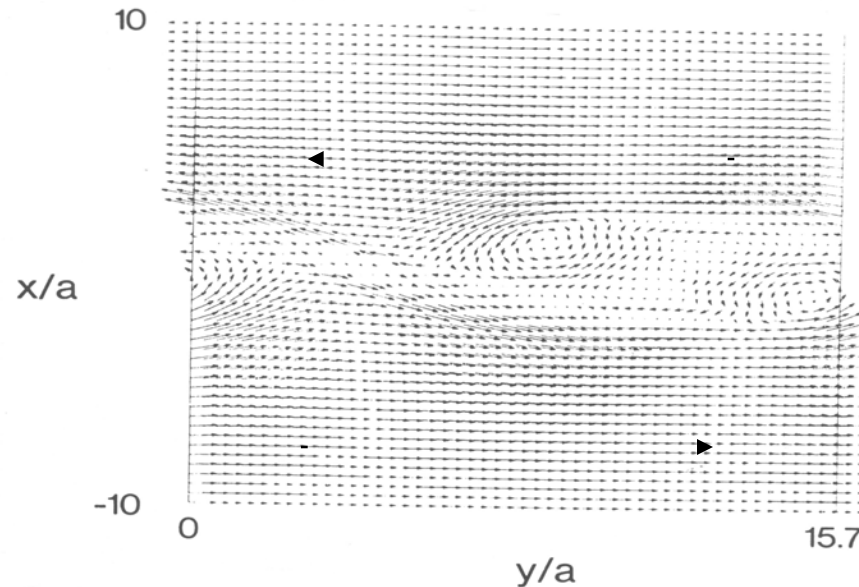
$$h\langle B\rangle\langle v_{\perp}\rangle \sim 25 \text{ kV}$$

If  $\langle B\rangle = 30 \text{ nT}$  and  $\langle v_{\perp}\rangle = 150 \text{ km/s}$  (slightly less than half the solar-wind speed),

$$h \sim 6000 \text{ km}$$

**Are there closed-model processes strong enough to create a closed-field-line boundary layer  $\sim 1 R_E$  thick?**

# Kelvin-Helmholtz Instability



(Miura, 1984)

- Kelvin-Helmholtz instability is driven by a velocity shear
  - Ideal-MHD instability
  - Causes crinkling of the boundary
  - Velocity swirls
  - Tends to be stabilized by different magnetic field directions on the sides of the shear
  - In nonlinear phase, causes macroscopic friction
  - Computer simulations suggest 10-30 kV potential drop across magnetosphere (maybe enough to explain quiet-time convection)

# Gradient/Curvature Drift Through Magnetopause

- The scale length  $L$  parallel to the boundary is  $\sim 10R_E$ .
- To form a boundary  $1 R_E$  thick about  $20 R_E$  behind Earth, the average gradient-drift speed would have to be at least  $\langle v_{\text{flow}} \rangle / 20$ , and  $\langle v_{\text{flow}} \rangle \sim v_{\text{flow}}$ . Therefore, the ratio in is too small by almost 2 orders of magnitude.
- Conclusion: Gradient drift doesn't transport particles fast enough drive observed convection under average conditions.

# Wave-Induced Diffusion Across the Magnetopause

- The magnetosheath has a lot of electromagnetic noise. Maybe that jiggles charged particles across field lines to form a thick boundary layer.
- **Bohm diffusion** (treatment from Hill, 1983):
  - To get an idea of how fast such wave-induced diffusion could possibly be, picture each wave-particle interaction as a collision. Assume the particle's velocity is completely randomized after each collision.
  - For the magnetopause boundary layer, put  $kT=200$  eV,  $B=20$  nT, and get a diffusion coefficient

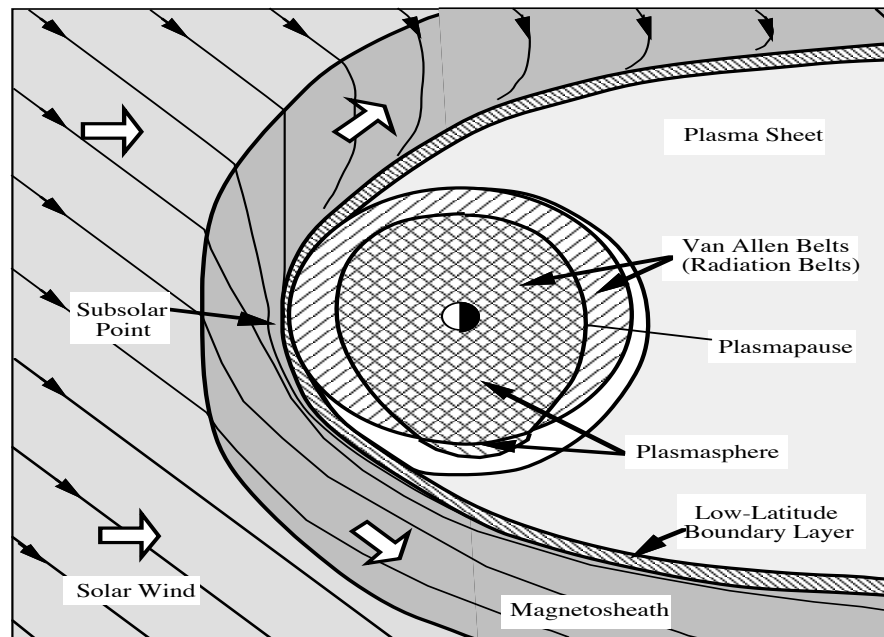
$$\sqrt{\langle \Delta x^2 \rangle} \sim \sqrt{2 \times 600 \times 1200} \sim 1200 km$$

- This is  $\sim$  one-fifth the boundary-layer thickness required to drive the average observed convection.

# Summary - closed transfer processes

- Optimistic estimate of Kelvin-Helmholtz provides < 40% of average drop
- Gradient drift provides ~10%
- Bohm diffusion (which is an upper limit) provides ~20%
- It's even harder to explain the potential drop observed in storms, which is ~ 4 times average.
- These estimates are rough, but they suggest that these closed-field-line transfer processes are not the primary drivers of convection.

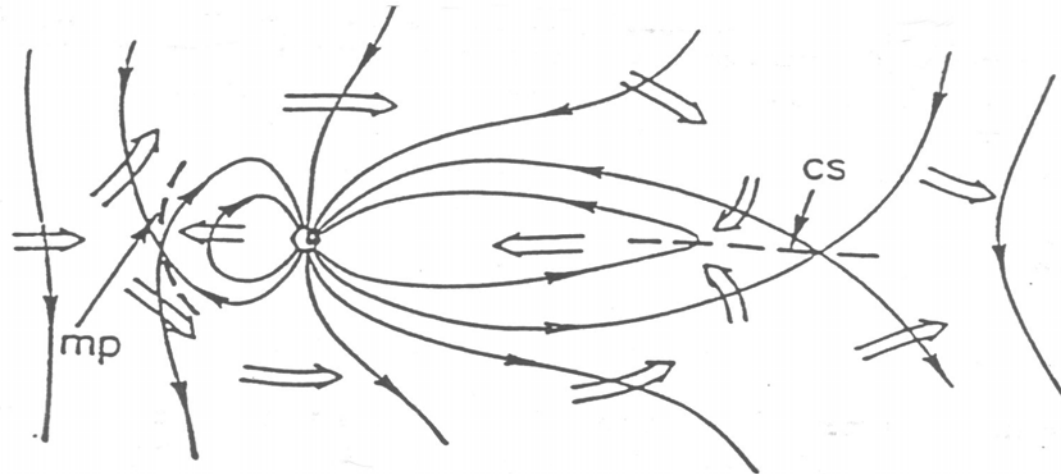
# Low-Latitude Boundary Layer



- Conventional wisdom is that much of the observed low-latitude boundary layer, which consists of antisunward-flowing plasma on the magnetopause, on northward-pointing magnetic fields, is driven by these closed-field-line transfer processes.
- These processes operate, but are not the primary drivers of convection.

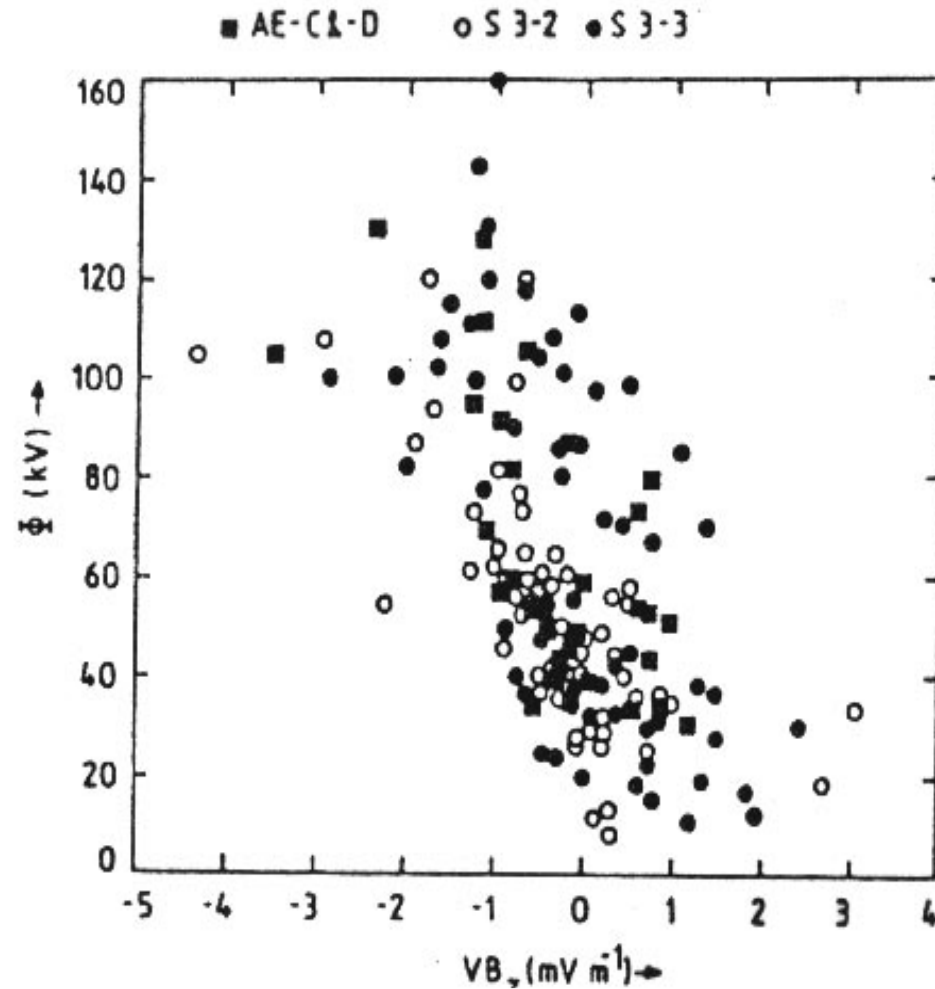
# Magnetic Reconnection

- Magnetic reconnection is the process whereby plasma  $\mathbf{E} \times \mathbf{B}$  drifts across a magnetic separatrix, i.e., a surface that separates regions containing topologically different magnetic field lines
  - (Vasyliunas, *Rev. Geophys. Space Phys.*, 13, 303, 1975)
  - In the original Dungey picture, reconnection occurs both on the dayside magnetopause and in the magnetotail.



# Empirical evidence

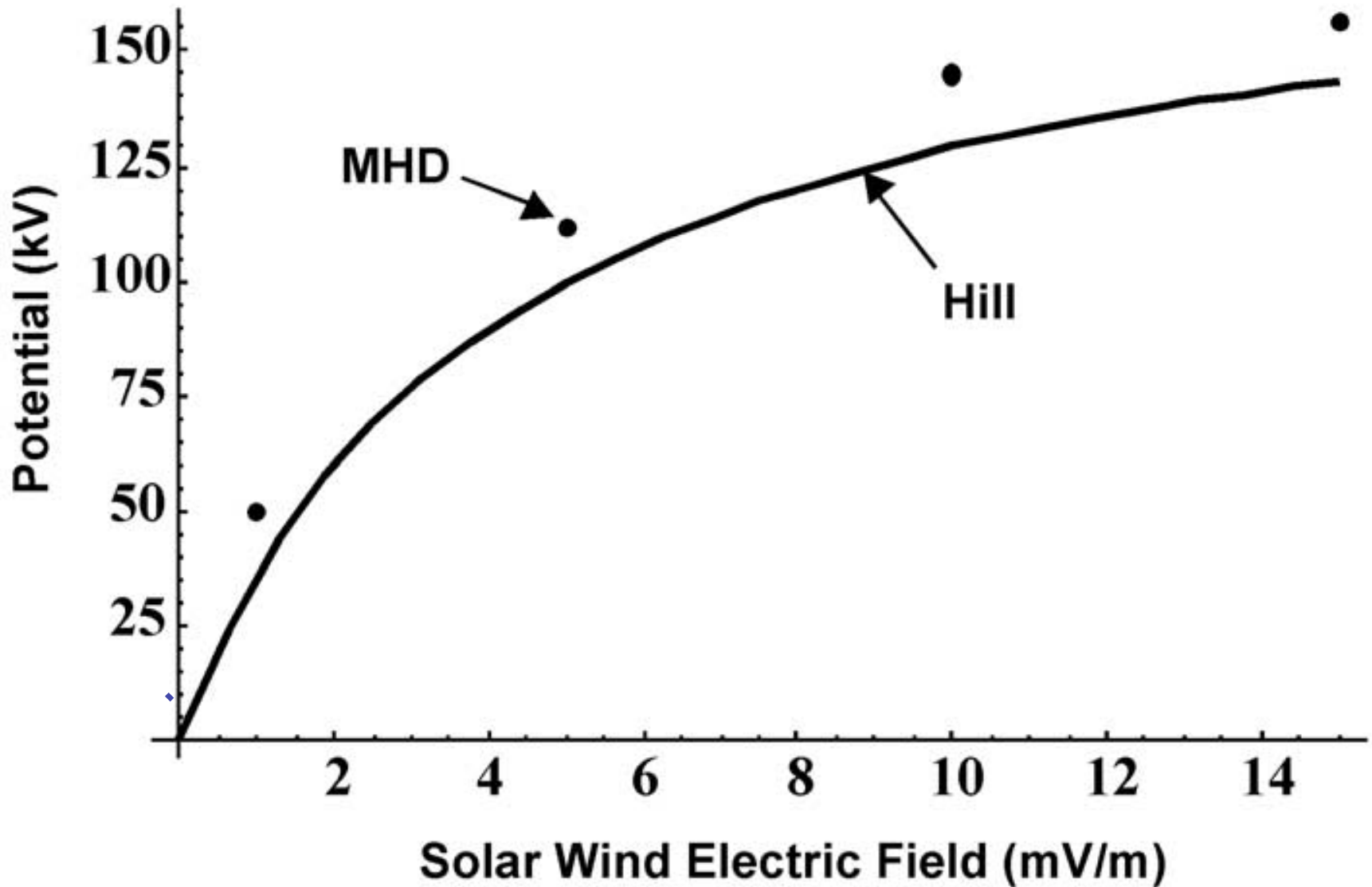
- Correlation of polar-cap potential drop with  $VB_z$  (From Reiff and Luhmann (1986))

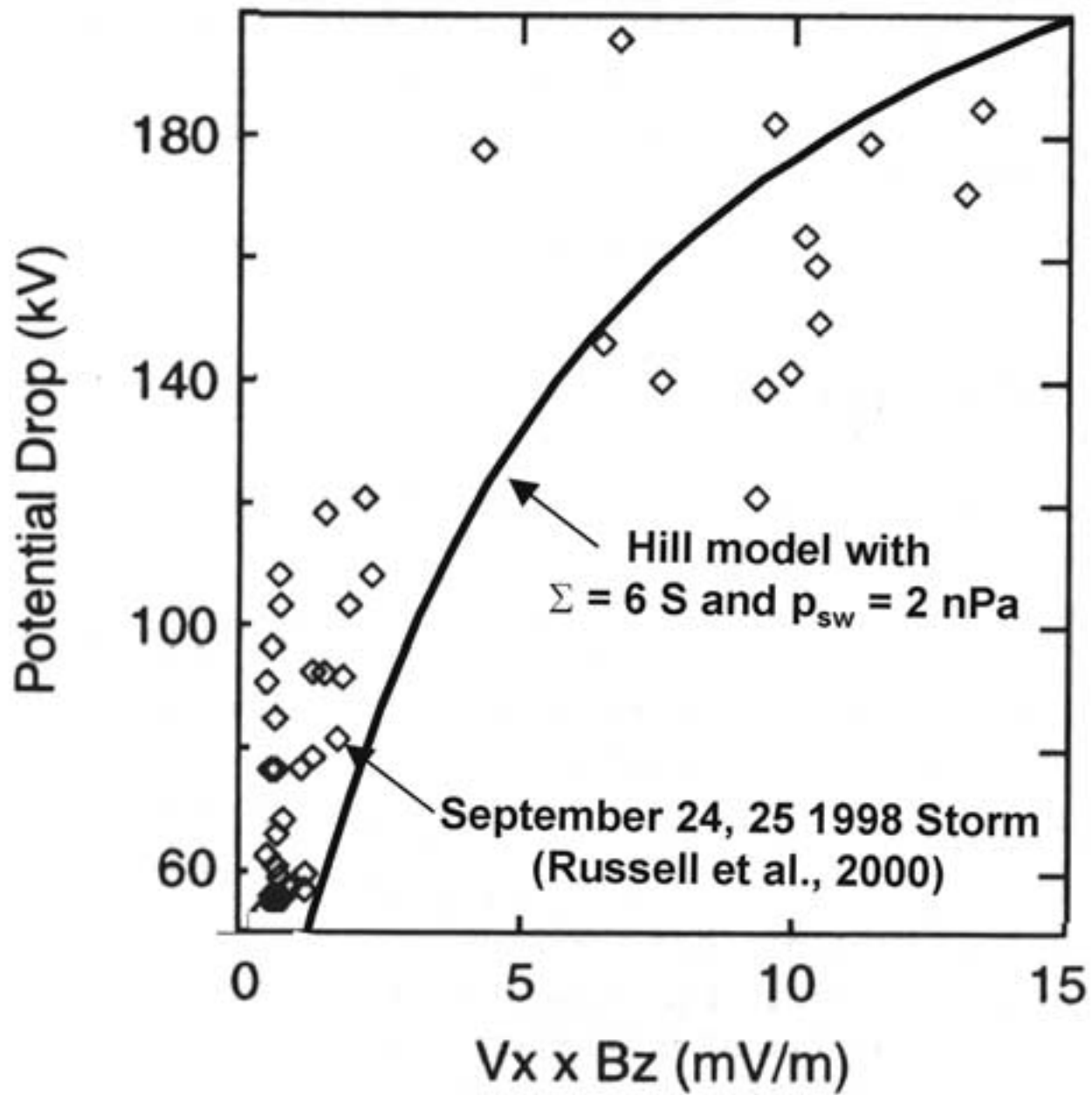


# Summary - Open Magnetosphere

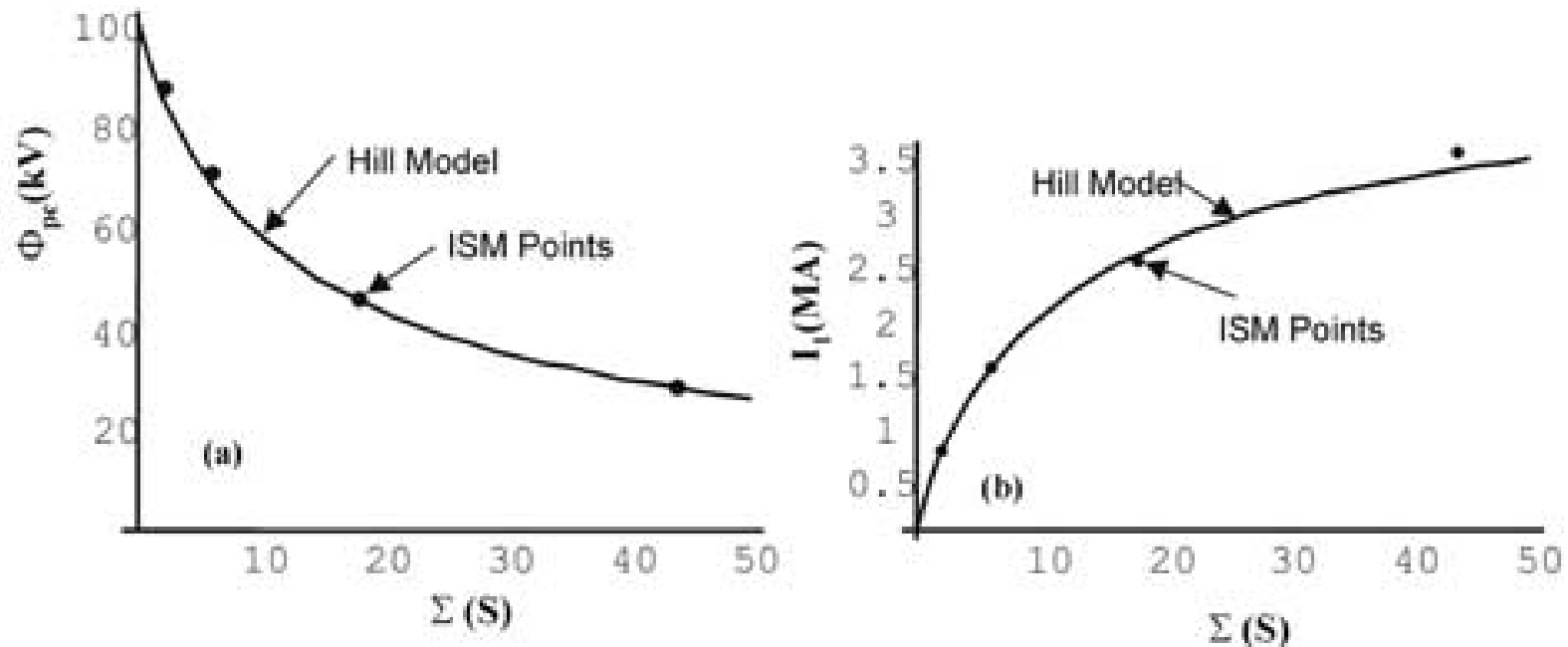
- The open model of the magnetosphere (Dungey, 1961) implied that convection would be strong for southward IMF
  - IMF is roughly anti-parallel to Earth's dipole
  - Facilitates reconnection at dayside magnetopause
- That basic prediction has been strongly confirmed.
- This was substantial evidence that reconnection at the dayside magnetopause was the dominant driver of magnetospheric convection.

# Polar Cap Saturation (Predicted by Hill, confirmed by simulations)



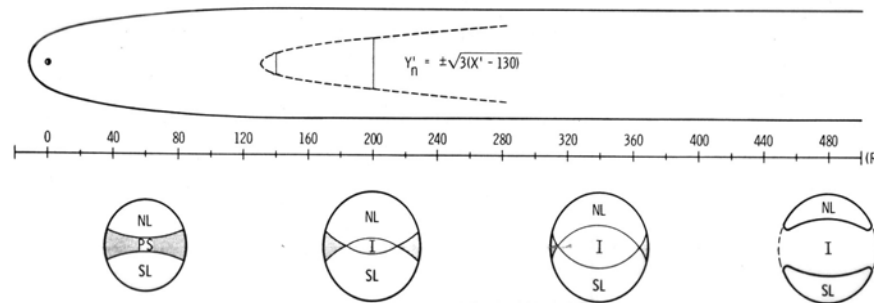


# Effect of Ionospheric Conductance



- The ionosphere plays an important role on determining the rate of convection on the ionosphere
  - The larger the conductance, the lower the convection rate

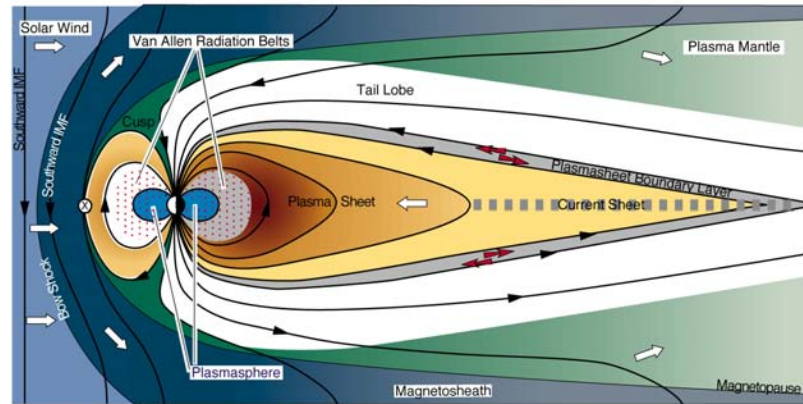
# Where Does Average $B_z$ Turn Negative?



Location of separatrix between interplanetary field lines and closed field lines, from Slavin et al. (1985).

- Neutral line of average  $B_z$ :
  - $\sim 130 R_E$  near local midnight
  - $\sim 300 R_E$  on the flanks
- The “wake”, which consists of field lines that are connected to the interplanetary medium on both “ends”, becomes a larger and larger part of the tail as you go downstream.

# Transfer of Particles into the Closed-Field-Line Region of the Magnetosphere



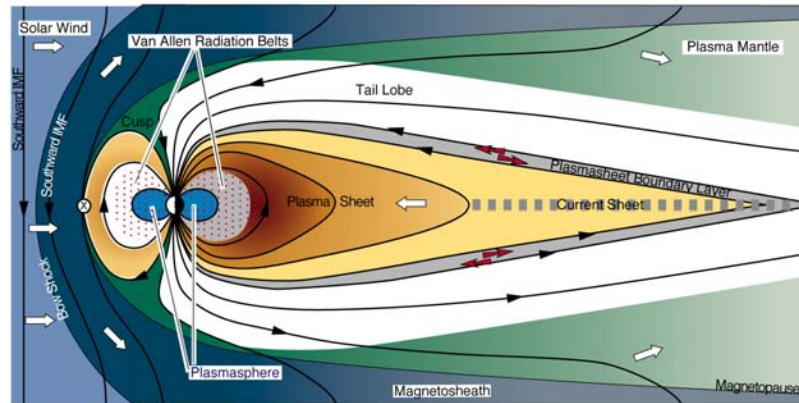
- Rate of earthward ion convection in the plasma sheet:  $\Phi_{ions}^{pl.sh.} \sim (1cm^{-3})(50km/s)(8R_E)(30R_E) \sim 5 \times 10^{26} s^{-1}$
- Solar-wind particles incident on the front of the magnetosphere:  $\Phi_{ions}^{solar\ wind} \sim (5cm^{-3})(400km/s)\pi(15R_E)^2 \sim 6 \times 10^{28} s^{-1}$
- Efficiency of particle penetration, assuming half the plasma sheet comes from the solar wind:

$$\eta_{ions} \sim \frac{\Phi_{ions}^{pl.sh.}}{2\Phi_{ions}^{solar\ wind}} \sim 0.004$$

# Question

- Roughly what is the total amount of mass in the magnetosphere?
  - $2 \times 10^{20}$  tons
  - $2 \times 10^{10}$  tons
  - 20 tons
  - $2 \times 10^{-12}$  tons

# Transfer of Energy into the Inner Magnetosphere/Ionosphere



- Rate of Joule dissipation in the ionosphere:  

$$\Phi_{energy}^{Joule\ heat} \sim (2\text{ hemispheres})(50,000\text{volts})(10^6\text{ A}) = 10^{11}\text{ watts}$$
- Estimated total dissipation in inner magnetosphere and ionosphere:  

$$\Phi_{energy}^{diss.} \sim 2 \times 10^{11}\text{ watts}$$
- Energy flux of solar wind times cross section of magnetosphere:  

$$\Phi_{energy}^{sw} \sim \left( \frac{n_{sw} m_i v_{sw}^3}{2} \right) \pi (15 R_E)^2 \approx \frac{(5\text{cm}^{-3})}{2} m_H (400\text{km/s})^3 \pi (15 R_E)^2 \sim 8 \times 10^{12}\text{ watts}$$
- Efficiency with which energy penetrates to the magnetospheric interior and ionosphere:  

$$\eta_{energy} = \frac{\Phi_{energy}^{dissipation}}{\Phi_{energy}^{sw}} \sim 0.025$$

## Transfer Efficiencies for Fluid Quantities

- Much more mass enters the plasma mantle and immediately escapes down the tail. That mass wasn't counted in the efficiency.
- Much more energy also enters the magnetosphere in the plasma mantle and escapes down the tail but wasn't counted in the efficiency. The loss of solar wind kinetic energy is estimated as

$$\begin{aligned}\Phi_{energy}^{sw \text{ to tail}} &\sim \frac{(B_{lobe})^2}{\mu_o} (v_{sw}) \pi (R_{tail})^2 / 2 \\ &\sim \frac{(20 \times 10^{-9} \text{ nT})^2}{\mu_o} (4 \times 10^5 \text{ m/s}) \pi (15 \times 6.37 \times 10^6 \text{ m})^2 / 2 \sim 3 \times 10^{12} \text{ watts}\end{aligned}$$

which is much larger than the energy dissipated in the ionosphere and magnetospheric interior.

# Energy Input - Poynting Flux

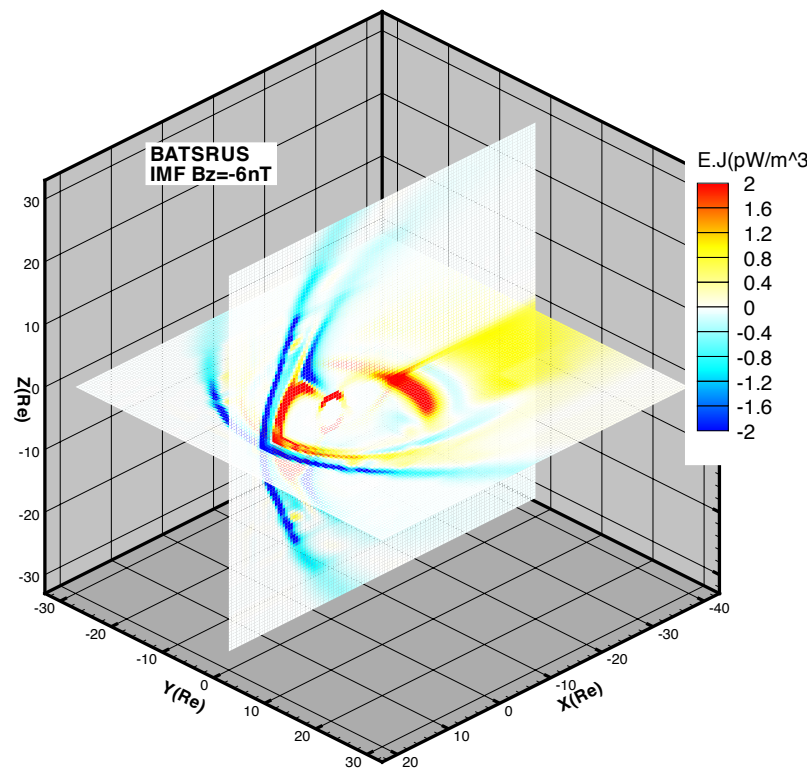
- It can be shown that the rate of conversion to/from mechanical energy from/to magnetic energy is given by (Hill, 1982)

$$\langle \mathbf{j} \cdot \mathbf{E} \rangle = - \langle \nabla \cdot (\mathbf{E} \times \mathbf{B}) / \mu_0 \rangle$$

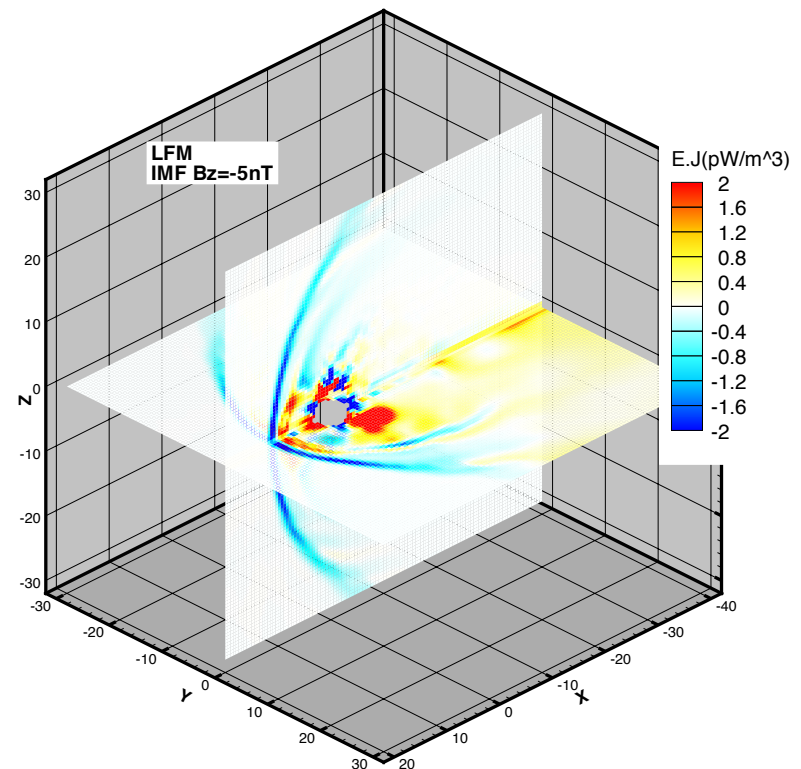
- Where  $\langle \rangle$  is a (sufficiently) long time average
- Basically, when
  - $\mathbf{j} \cdot \mathbf{E} > 0$ , magnetic energy is converted to flow energy
  - $\mathbf{j} \cdot \mathbf{E} < 0$  flow energy is converted to magnetic energy

# Example from Global MHD - Southward IMF

**SWMF**

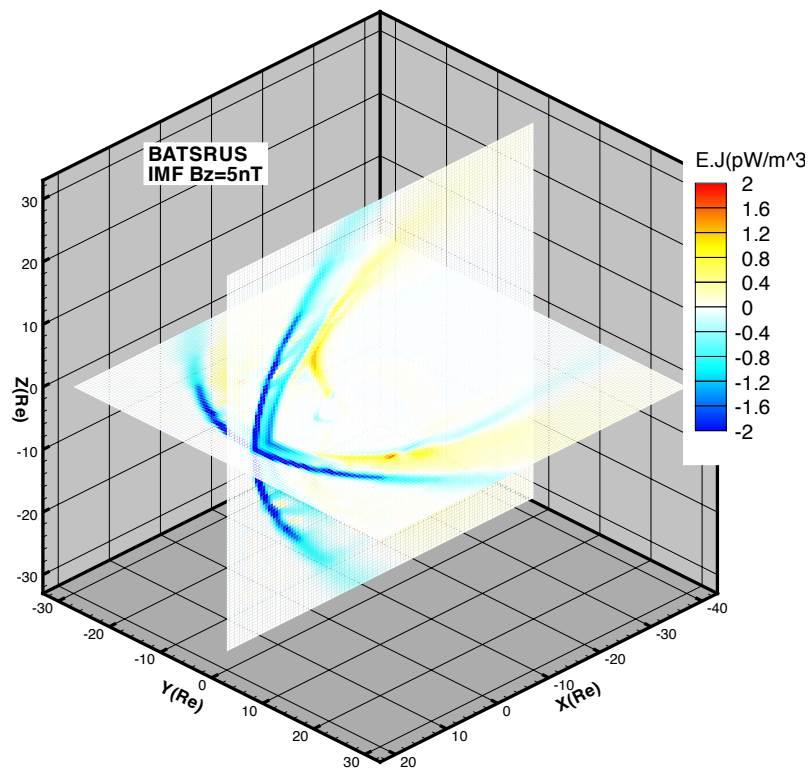


**LFM**

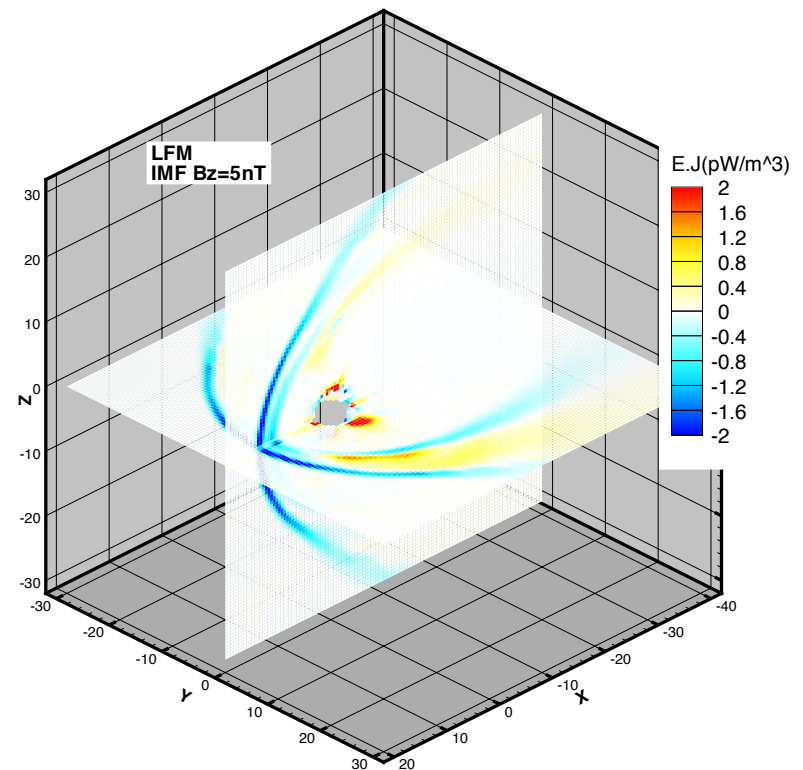


# Example from Global MHD – Northward IMF

**SWMF**



**LFM**



# Momentum Coupling

- How does the force applied by solar wind manifest itself in the magnetosphere?
  - At the magnetopause, both normal and tangential forces are acting
  - The normal force is the solar wind ram pressure is

*Ram force  $\sim$  ram pressure  $\times$  area presented to the SW*

$$\sim (5 \text{ cm}^{-3})(1.67 \times 10^{-27} \text{ kg})(400 \text{ km / s})^2 \pi(15R_E)^2$$

$$\sim 4 \times 10^7 \text{ N}$$

# Question

- Which is larger?
  - Solar wind dynamic pressure?
  - Solar radiation pressure?

# Question

- Which is larger
  - Solar wind dynamic pressure?  $\sim 2 \times 10^{-9}$  Pa
  - Solar radiation pressure?  $\sim 5 \times 10^{-6}$  Pa

# Question

- Which is larger
  - Solar wind dynamic force?
  - Solar radiation force?

# Question

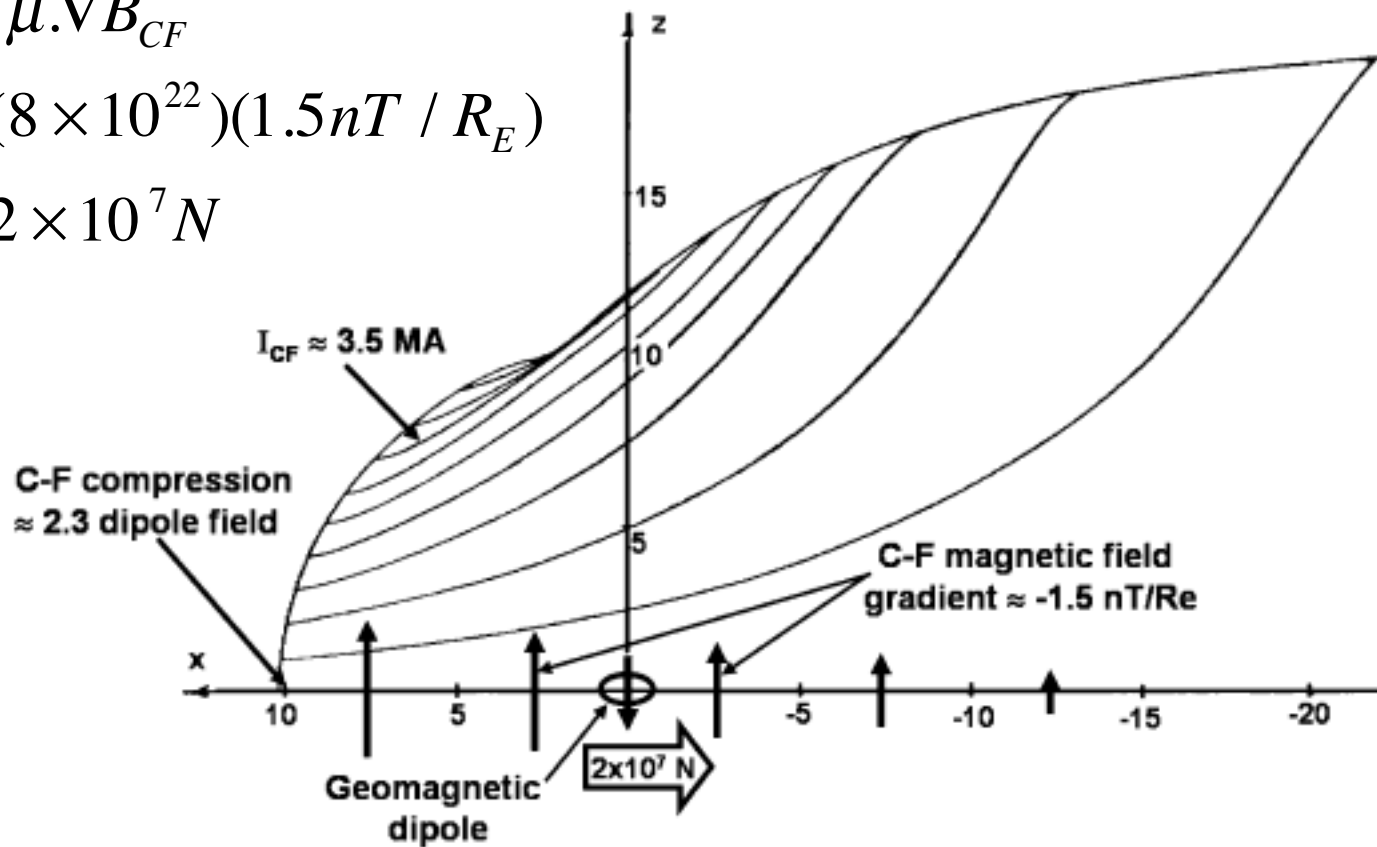
- Which is larger
  - Solar wind dynamic force?  $\sim 2 \times 10^7$  N
  - Solar radiation force?  $\sim 6 \times 10^8$  N

# Comment on Forces

- With a force  $\sim 10^7$  N, the  $\sim 200+$  tons of plasma in the magnetosphere would be blown down the tail
- Ultimately the only mass able to hold off the force is the Earth itself [*Vasyliunas, 2007*]

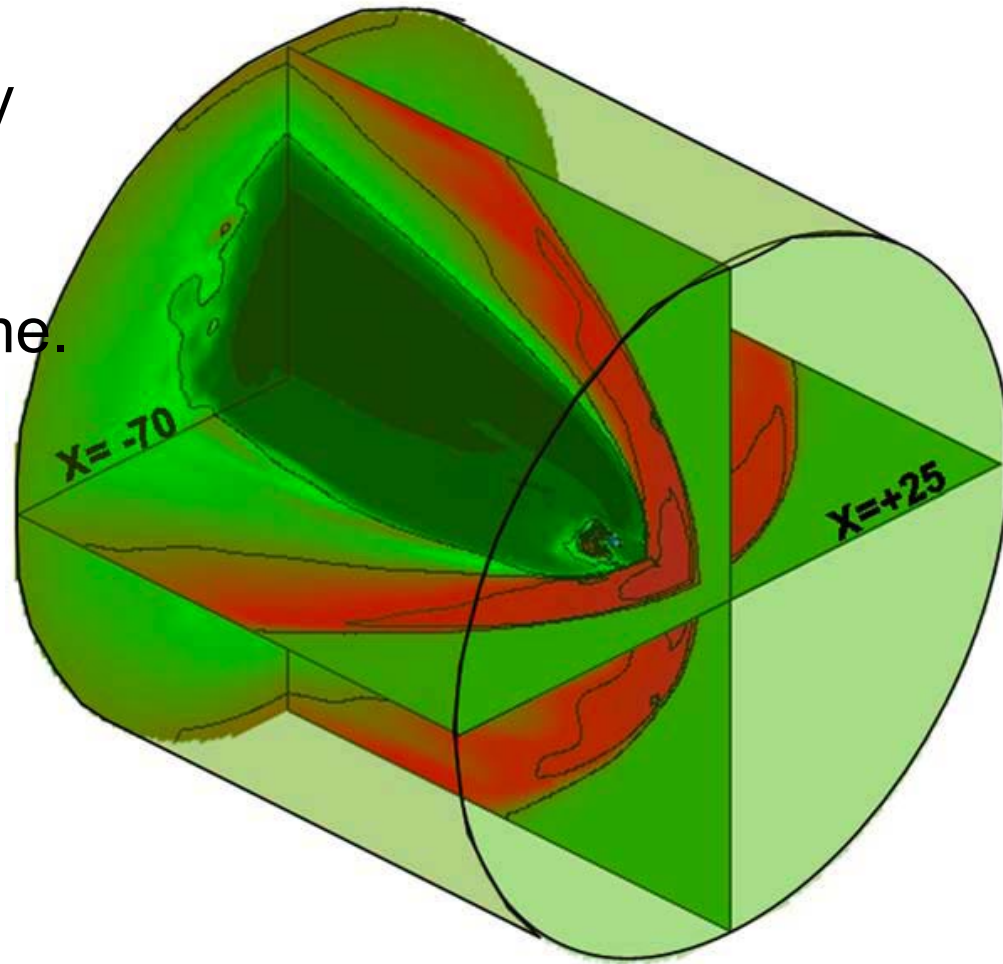
# Force of Chapman-Ferraro Current on the dipole

$$\begin{aligned} F_{CF} &\approx \mu \cdot \nabla B_{CF} \\ &\approx (8 \times 10^{22}) (1.5 \text{ nT} / R_E) \\ &\approx 2 \times 10^7 \text{ N} \end{aligned}$$

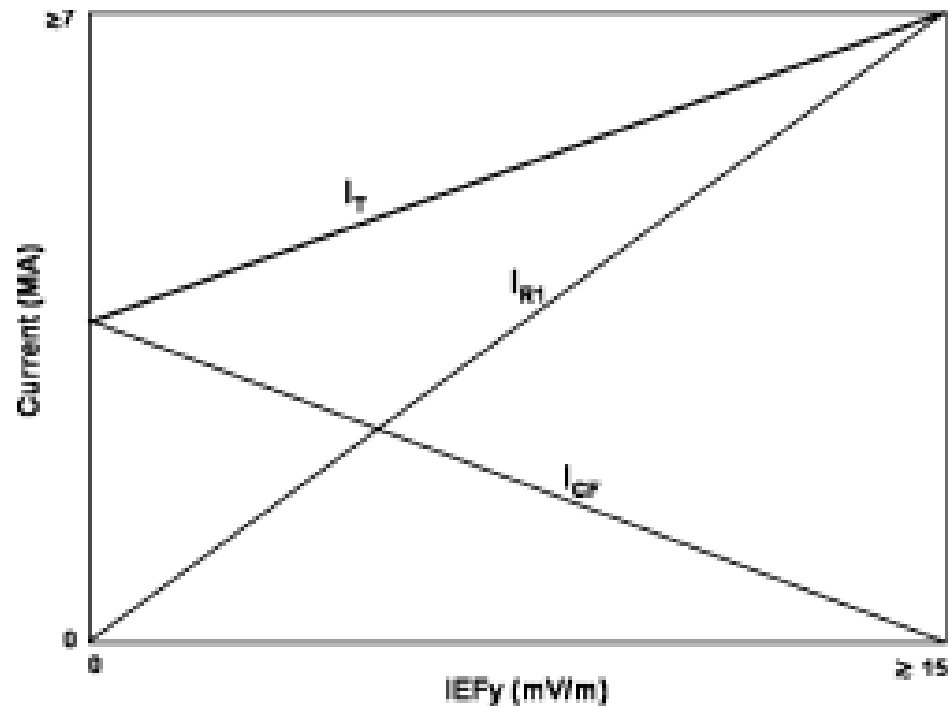


# From Global MHD

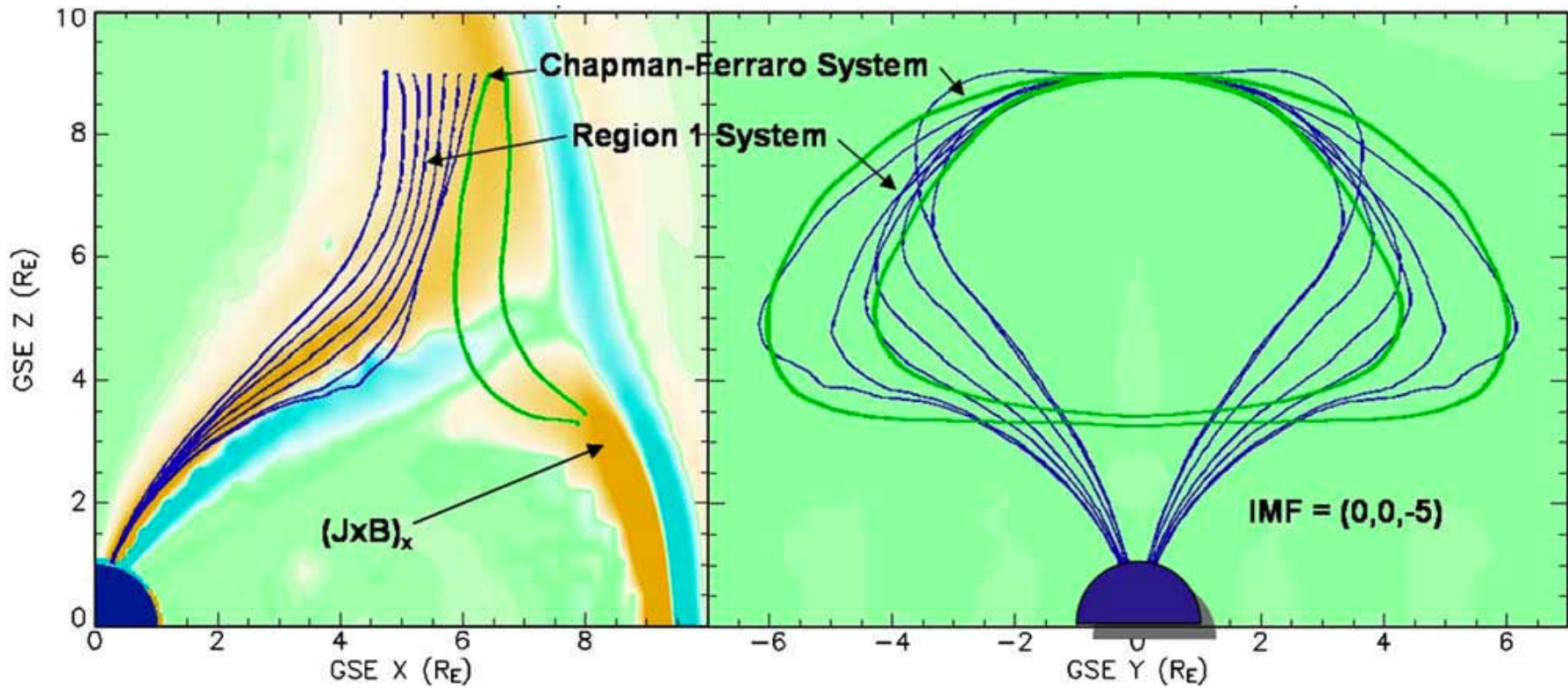
Siscoe and Siebert,  
2006 got  $2.4 \times 10^7 \text{N}$  by  
integrating the  
momentum stress  
tensor over the volume.



# Changes of Chapman Ferraro and R-1 currents with increasing IMF $E_y$ .

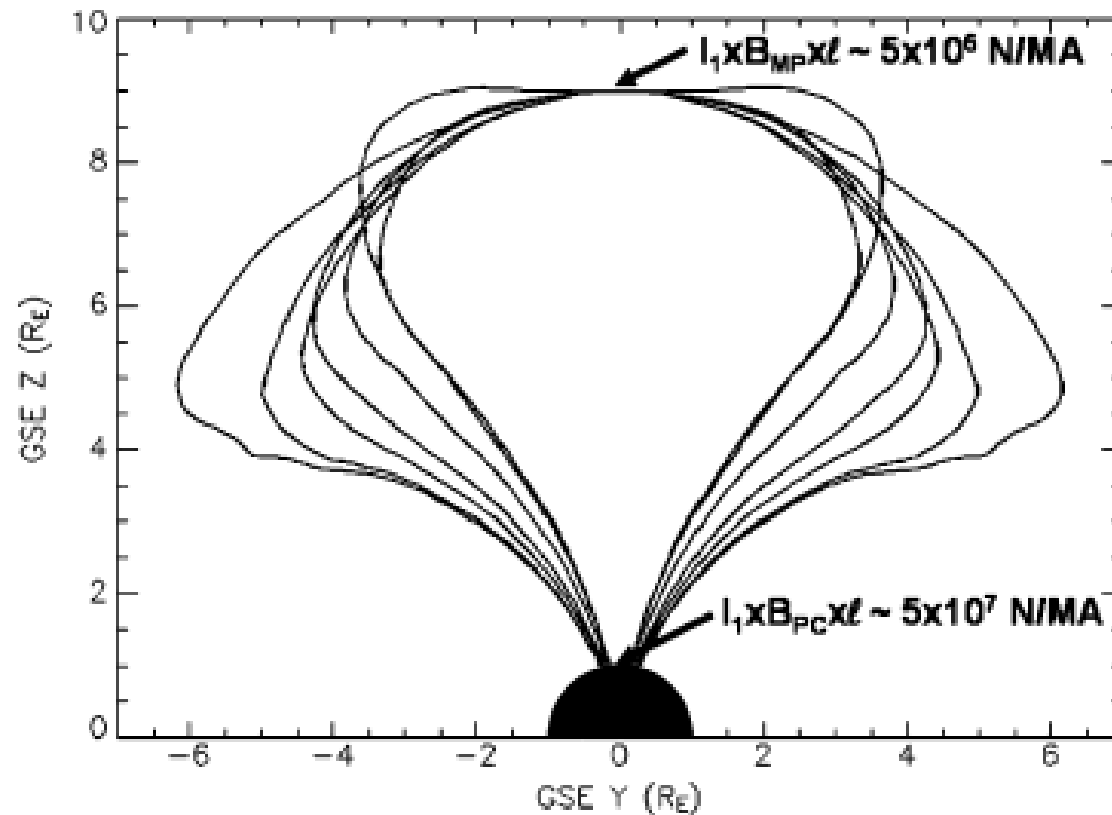


# Force



Tan=positive, blue=negative

# Tailward force on the thermosphere exceeds solar wind drag



This was also noted by Hill, 1982 and discussed in detail by Vasyliunas, 2007

# Comments on Transfer Efficiencies for Fluid Quantities

- Efficiency of momentum transfer:

$$\frac{\textit{Drag}}{\textit{Ram force}} \sim \frac{\frac{(20 \textit{nT})^2}{2\mu_o}}{(5 \textit{cm}^{-3})(1.67 \times 10^{-27} \textit{kg})(400 \textit{km/s})^2}} \sim 0.12$$

where the numerator is an estimate of the tension force per unit area on the tail.

# Penetration of Solar-Wind Magnetic Flux into Magnetotail

- Magnetic flux:

- The magnetic flux in the polar cap (or tail lobes) is estimated as

$$\Phi_{Bn}^{pc} \sim \pi \left( \frac{15^\circ}{57.296^\circ} \right)^2 (6.27 \times 10^6 m)^2 (5 \times 10^{-4} T) \sim 4.4 \times 10^8 Wb$$

These magnetospheric field lines are all connected to the solar wind and thus represent the effects of reconnection.

- The magnetic flux that would thread through the region occupied by the magnetotail, if the magnetotail weren't there is estimated as

$$\Phi_{Bn}^{sw} \sim 40 \times 30 \times 300 \times (6.37 \times 10^6 m)^2 \times (5 \times 10^{-9} T) \sim 2.4 \times 10^9 Wb$$

so the the efficiency with which the magnetic field gets across the tail magnetopause is estimated as

$$\eta_{Bn} \sim \frac{\Phi_{Bn}^{pc}}{\Phi_{Bn}^{sw}} \sim 0.18$$

# Penetration of $E_y$ into Magnetosphere in Times of Southward IMF

- The average observed polar cap potential drop in times of southward IMF is given roughly by

$$\Phi_{Ey}^{pc} \sim 80 \text{ kV}$$

- The average potential drop across a distance of  $30 R_E$  (diameter of dayside magnetopause) would be  $\Phi_{Etan}^{sw} \sim v_{sw} B_{sw} (30 R_E) \sim (400 \text{ km/s})(5 \text{ nT})(30 \times 6.37 \times 10^6) \sim 382,000 \text{ V}$

The implied efficiency is

$$\eta_{Etan} = \frac{\Phi_{Etan}^{pc}}{\Phi_{Etan}^{sw}} \sim 0.21$$

# Summary Comments on Efficiency

- Only a small fraction ( $\sim 1\%$ ) of the total particles and energy incident on the dayside magnetopause gets into the inner and middle magnetosphere, where there is sunward convection.
- A much larger fraction of the solar wind particles and momentum convect through the plasma mantle but never get deeply involved in the life of the magnetosphere.
- About 10-20% of the solar wind electric field penetrates, in times of southward IMF.

# Global MHD models

- Global MHD models are now able to reproduce many of the global quantities discussed above
- However they often don't get the exact same results for the same inputs
  - Probably due to numerics such as resolution, numerical methods, etc
- While they seem to do a good job getting the gross scale physics correct, there is a lot of missing physics in the models
  - e.g, microphysics of reconnection, drift physics, etc
  - There has been efforts in the past few years to incorporate missing physics in the models

# Essential requirements to successful MHD Modeling

- Requirements include
  - Accurate solution of the MHD equations
    - Quite difficult, due to the nature of the MHD equations
      - That said, it is the violation of the ideal MHD requirement that drives the system
    - Keeping divergence of B requires special techniques
  - Accurate modeling of the bow shock and boundaries such as the magnetopause
  - Proper representation of the boundary conditions
    - Outer boundary is placed in the supersonic regime to eliminate any artifacts
    - Inner boundary, near the Earth should represent the effects of coupling to the ionosphere which requires an ionospheric model
  - Challenges in regions where wave speed get very large (effects model timestep)
    - Near the Earth, where the magnetic field gets large
    - In the lobes, where the density is low

# Global MHD Models at CCMC

Model	When Developed	Grid	Institution	Numerical Method	Divergence of B
LFM/CMIT	mid 80's	Stretched Polar	CISM	Partial Interface method	Yee grid
OpenGGCM	mid 90's	Stretched Cartesian	UNH	Hybrid Harten method	Yee grid
SWMF	late 90's	Cartesian using AMR	CSEM	Godunov method	Various, including advection

# MHD Equations (from Lyon et al, 2004)

$$\frac{\partial \rho}{\partial t} + \nabla \cdot (\rho \vec{v}) = 0$$

$$\frac{\partial(\rho \vec{v})}{\partial t} + \nabla \cdot [\rho \vec{v} \vec{v} + \mathbf{I}(P + \frac{B^2}{2\mu_0}) - \frac{\vec{B}\vec{B}}{\mu_0}] = 0$$

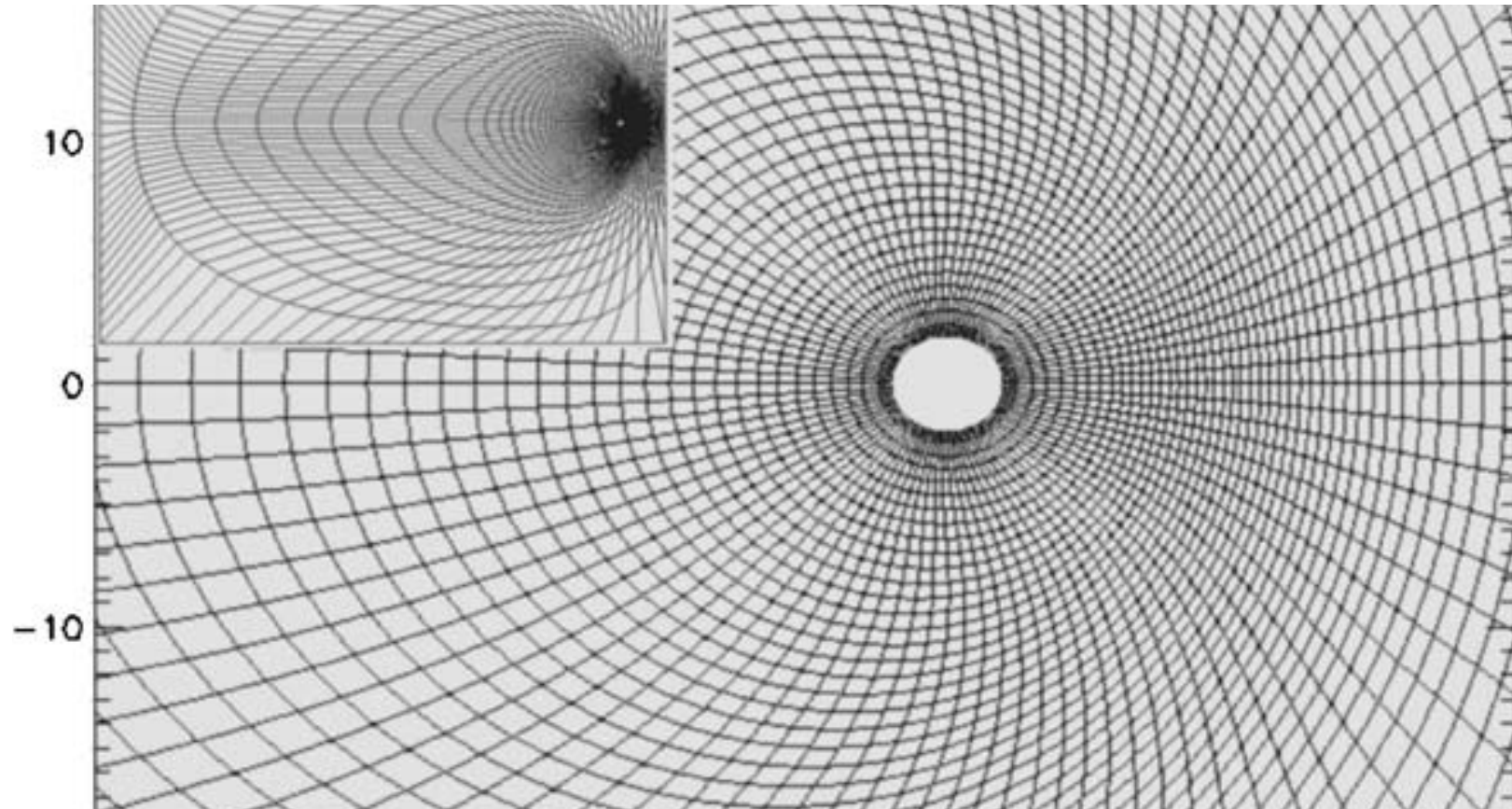
$$\frac{\partial E}{\partial t} + \nabla \cdot [\vec{v}(\frac{\rho v^2}{2} + \frac{\gamma}{\gamma-1} P)] + \vec{v} \cdot \nabla \cdot [\mathbf{I} \frac{B^2}{2\mu_0} - \frac{\vec{B}\vec{B}}{\mu_0}] = 0$$

$$\frac{\partial \vec{B}}{\partial t} - \nabla \times (\vec{v} \times \vec{B}) = 0$$

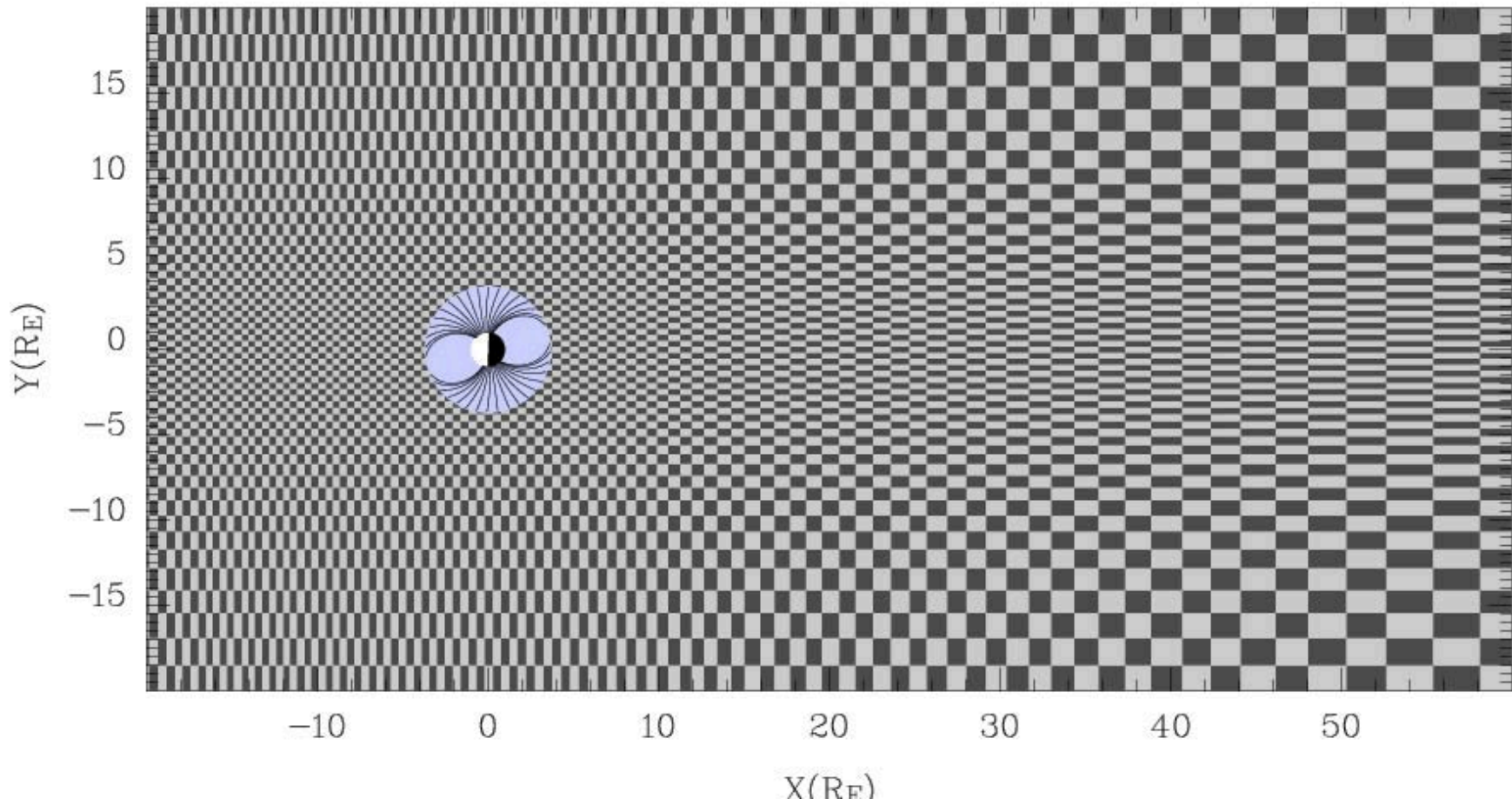
$$E = \frac{\rho v^2}{2} + \frac{1}{\gamma-1} P$$

$$\nabla \cdot \vec{B} = 0$$

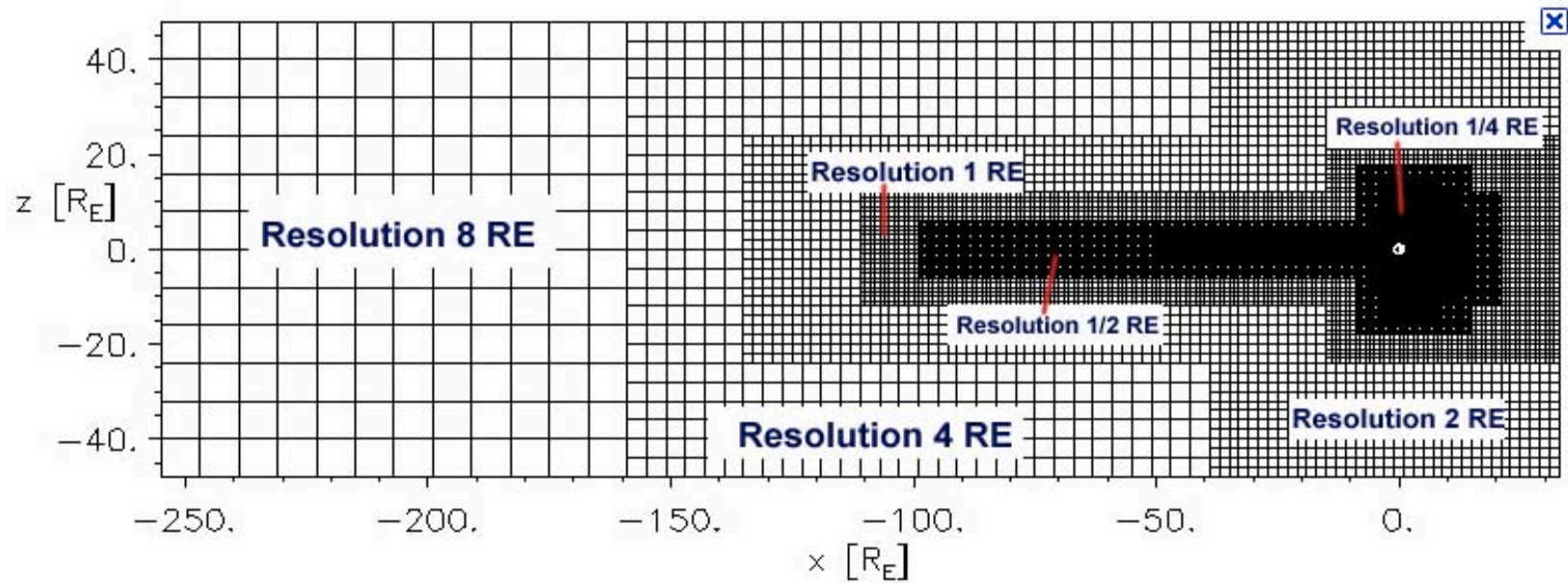
# LFM Grid – Stretched Polar Grid

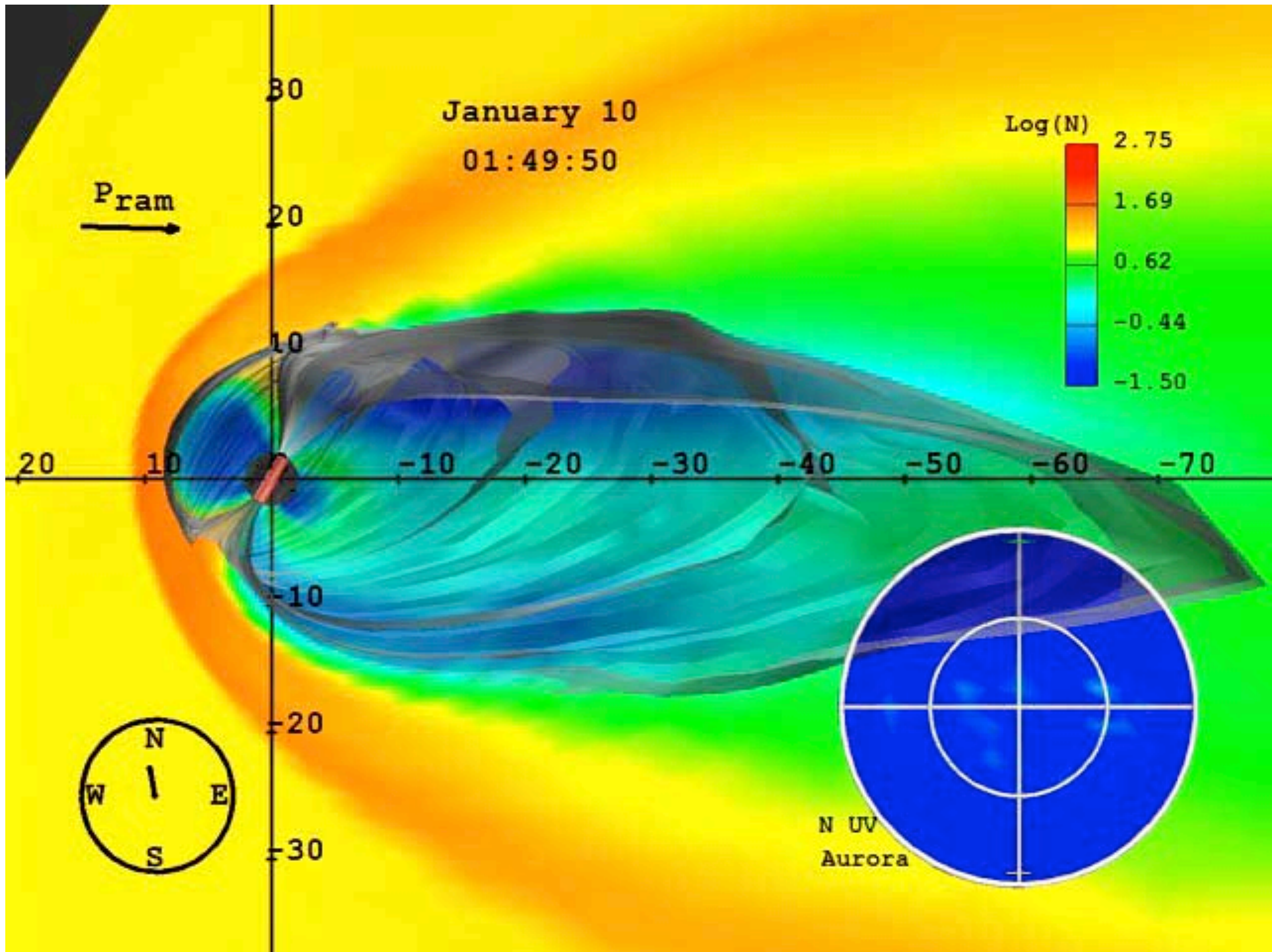


# OpenGGCM Grid

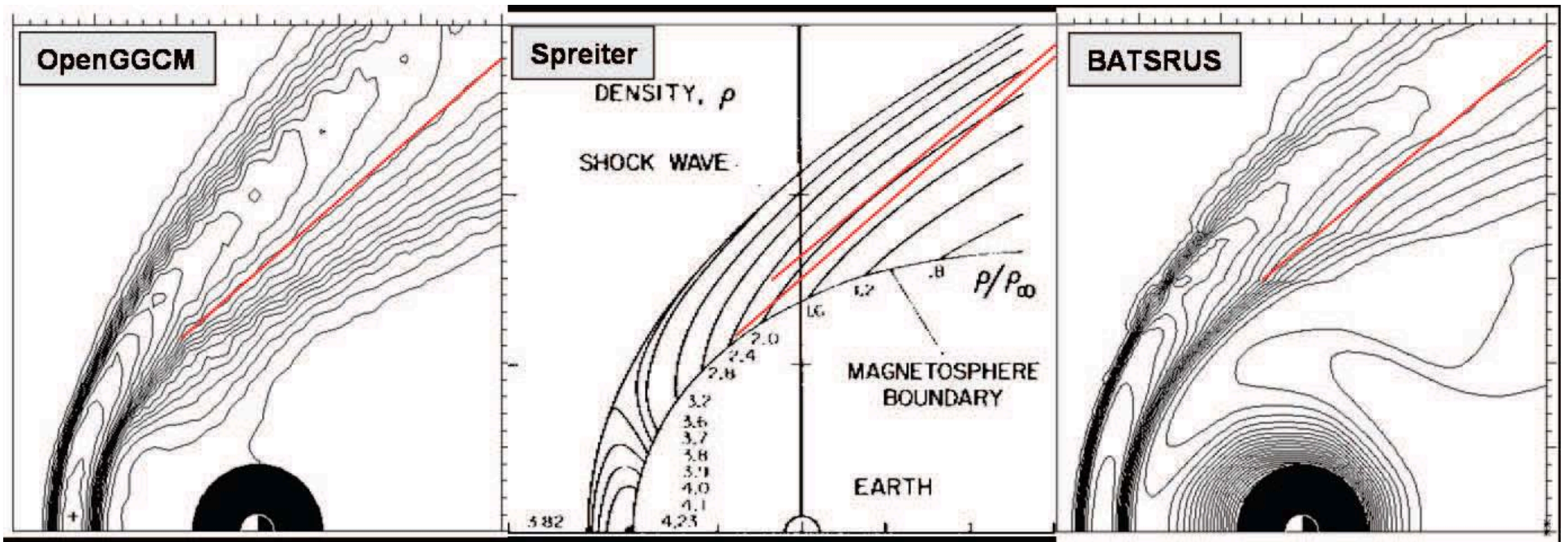


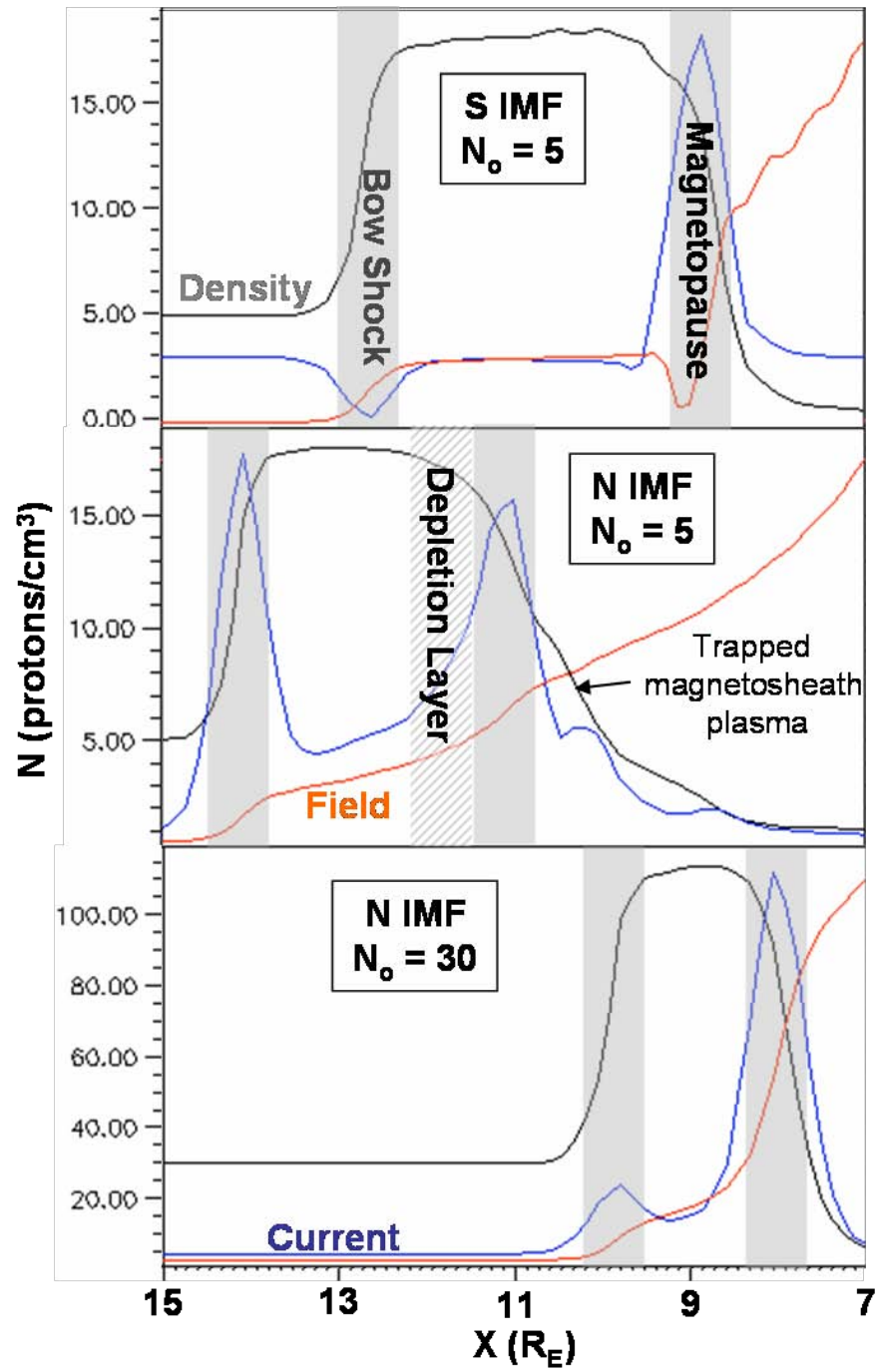
# SWMF Grid (from CCMC website)





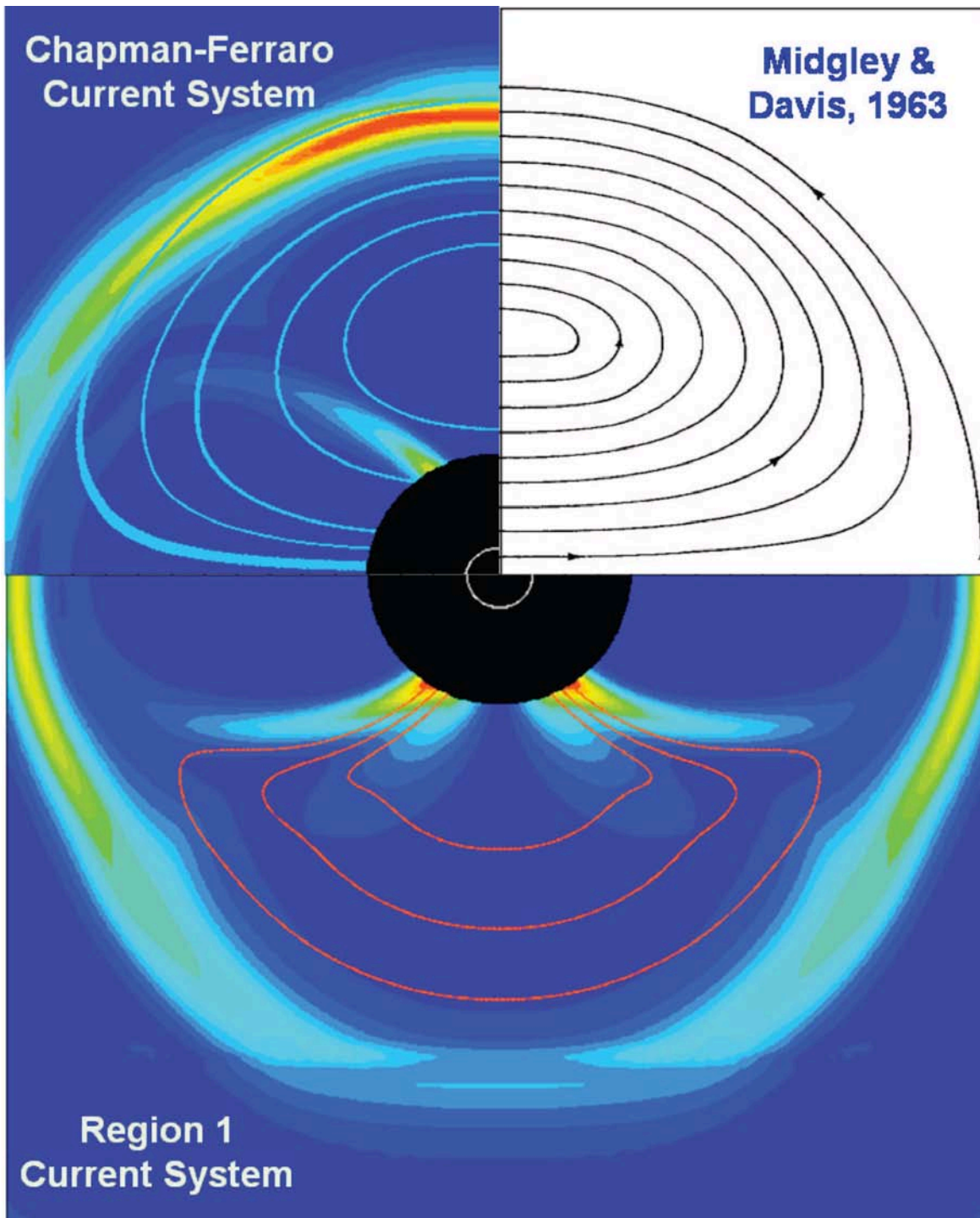
# Magnetosheath comparison





**Chapman-Ferraro  
Current System**

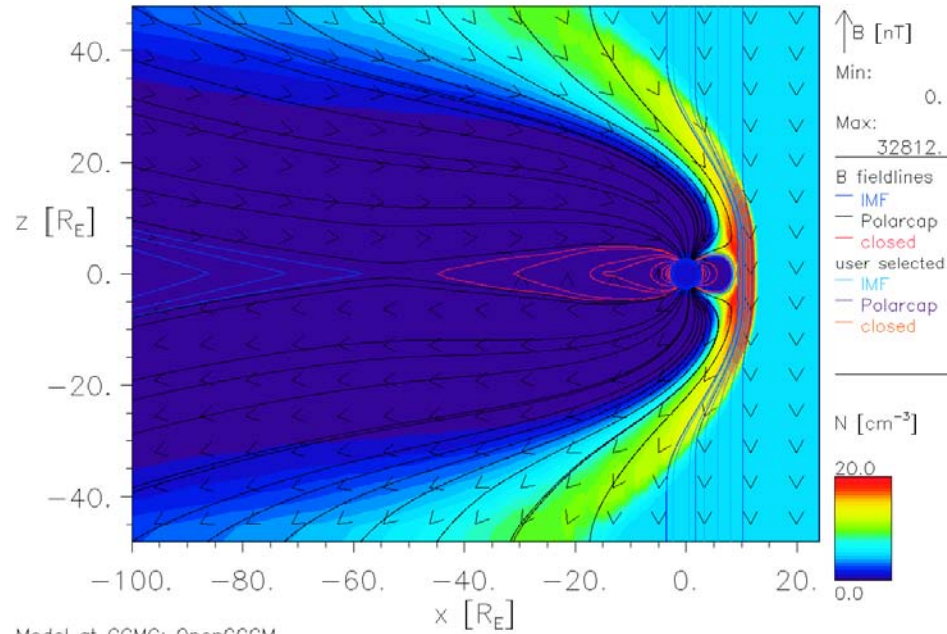
**Midgley &  
Davis, 1963**



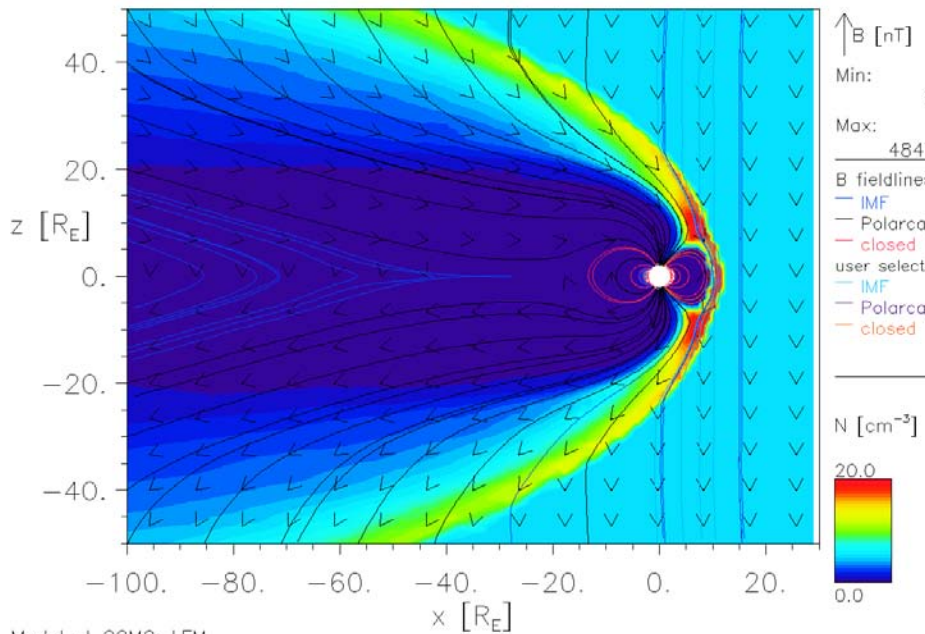
**Region 1  
Current System**

**IMF**  
 **$B_z = -5\text{nT}$**

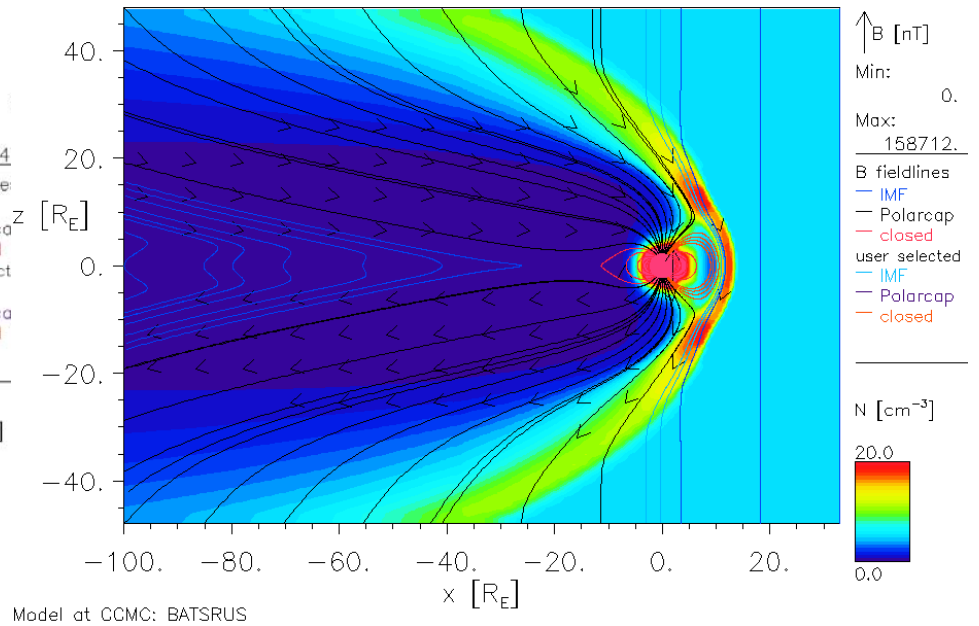
01/01/2000 Time = 02:00:00 UT  $y = 0.00R_E$



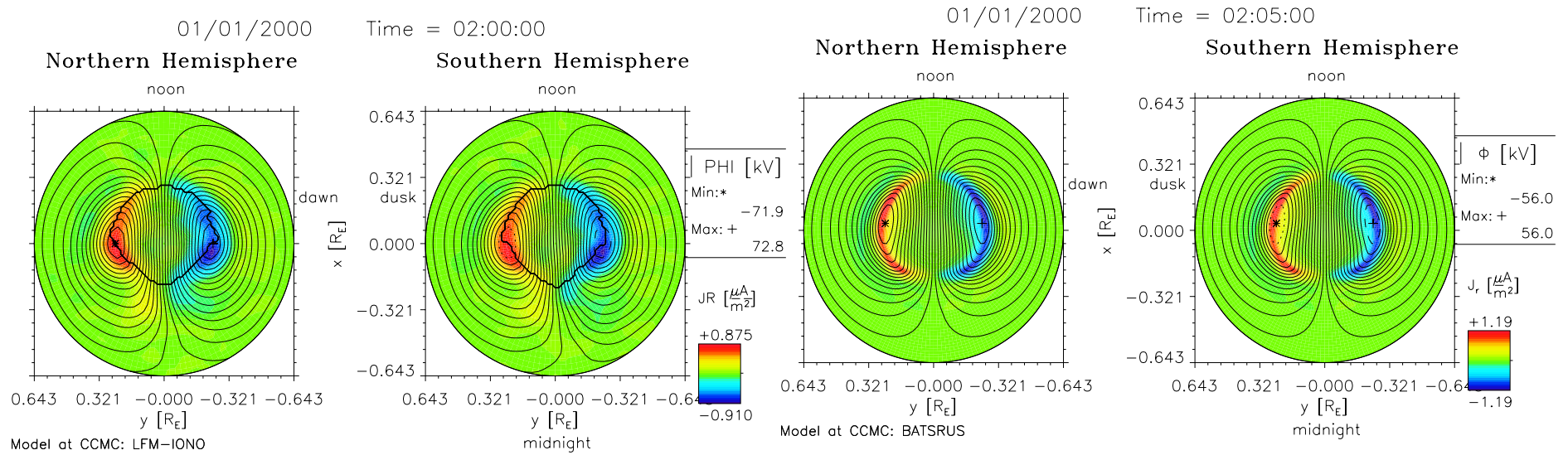
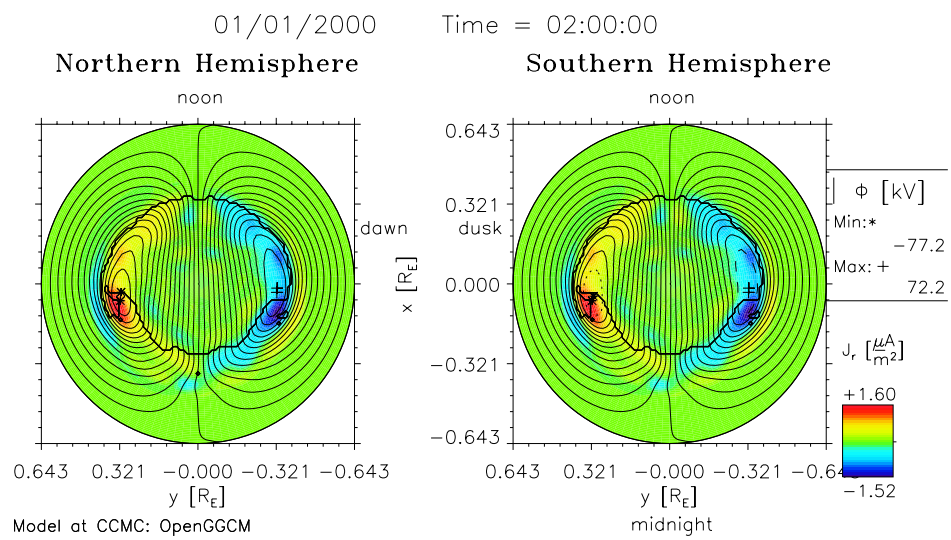
01/01/2000 Time = 02:00:00 UT  $y = 0.00R_E$

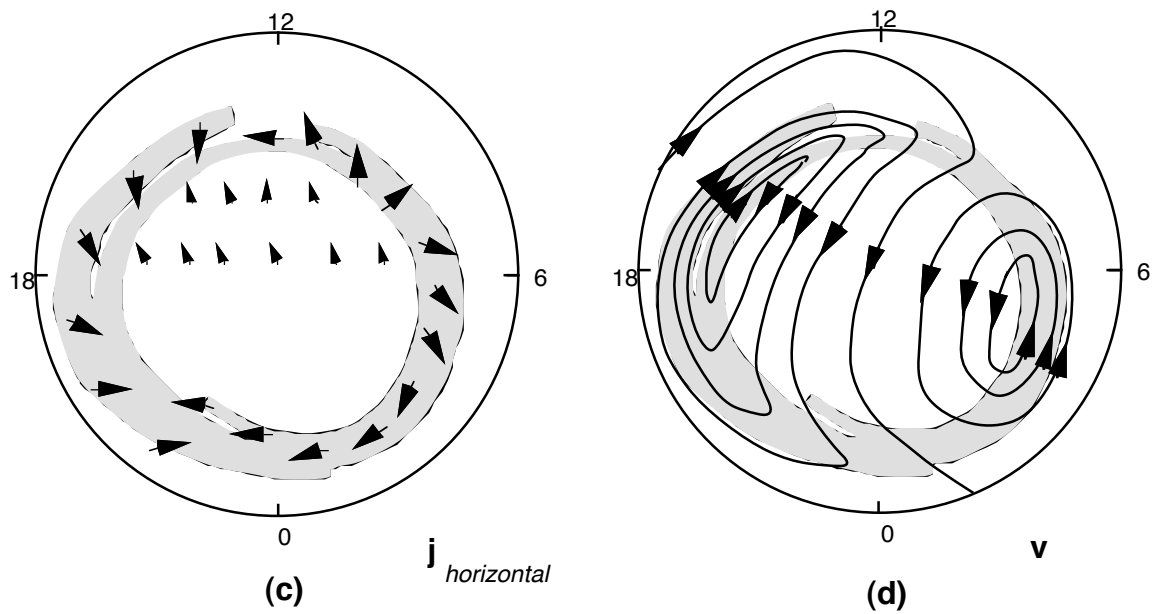
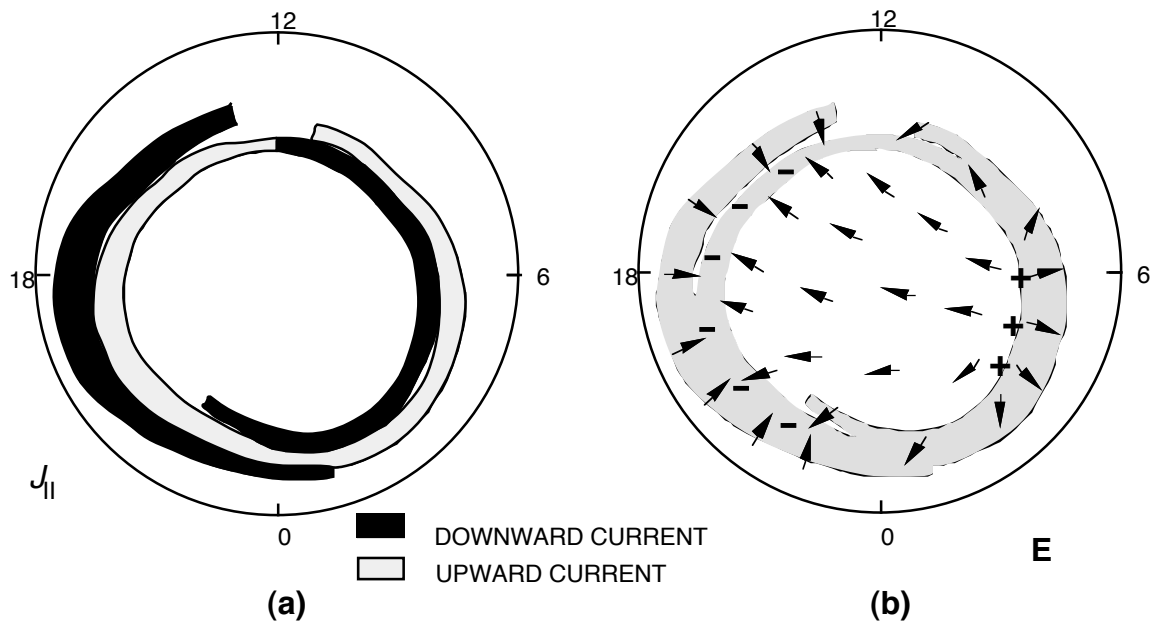


01/01/2000 Time = 02:00:00 UT  $y = 0.00R_E$



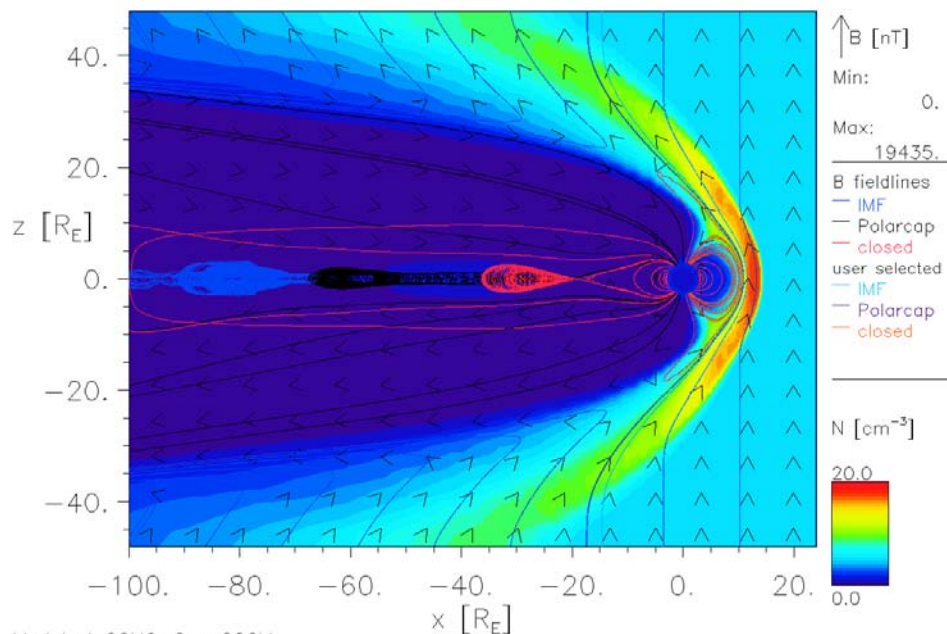
**IMF**  
 $B_z = -5\text{nT}$





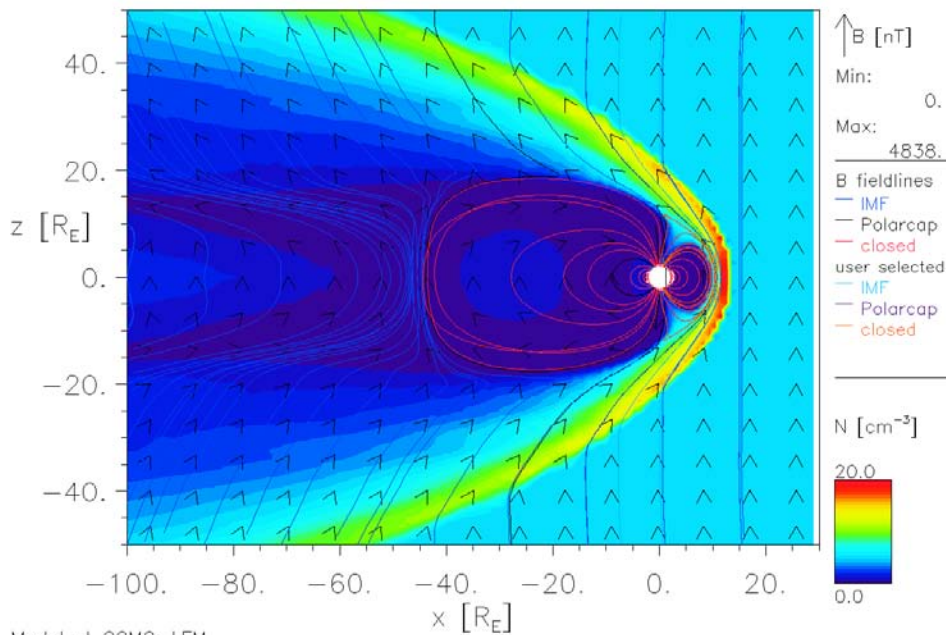
**IMF  $B_z = 5\text{nT}$**

01/01/2000 Time = 02:00:00 UT  $y = 0.00R_E$



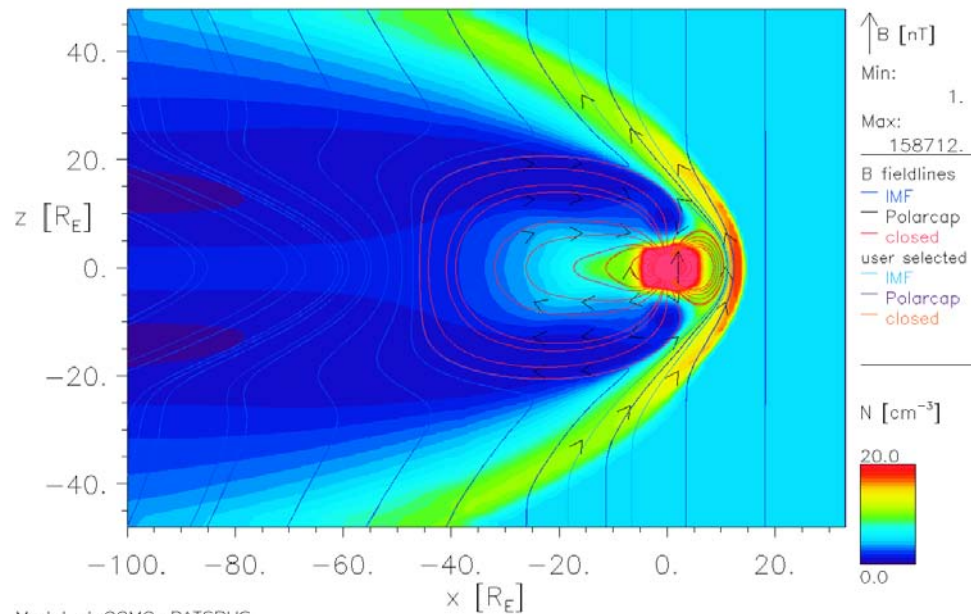
Model at CCMC: OpenGGCM

01/01/2000 Time = 02:00:00 UT  $y = 0.00R_E$



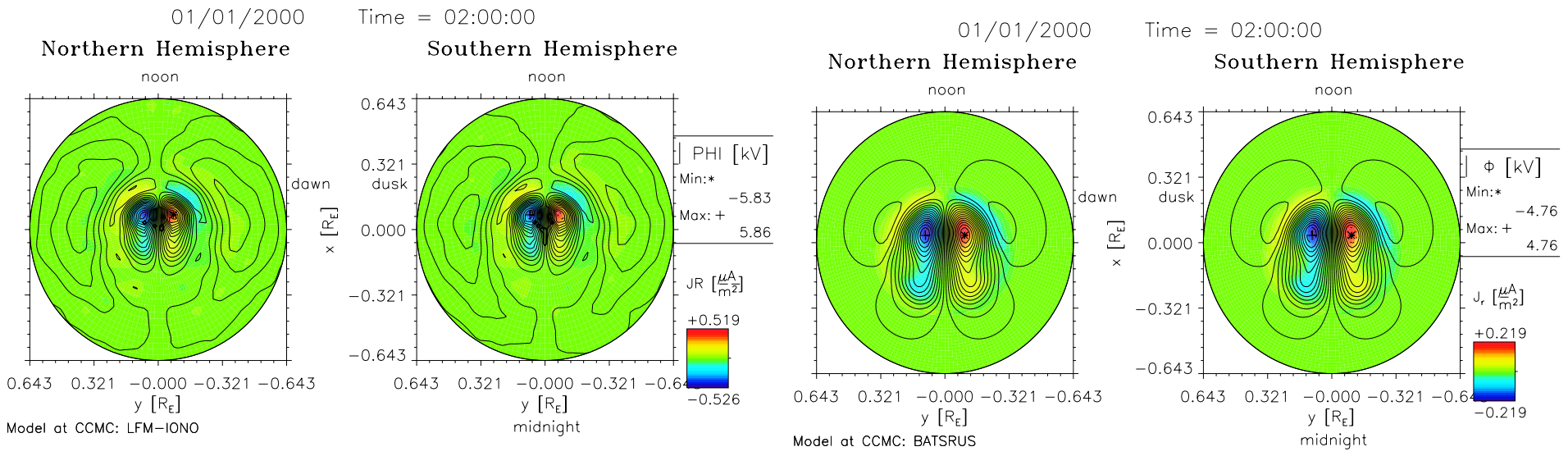
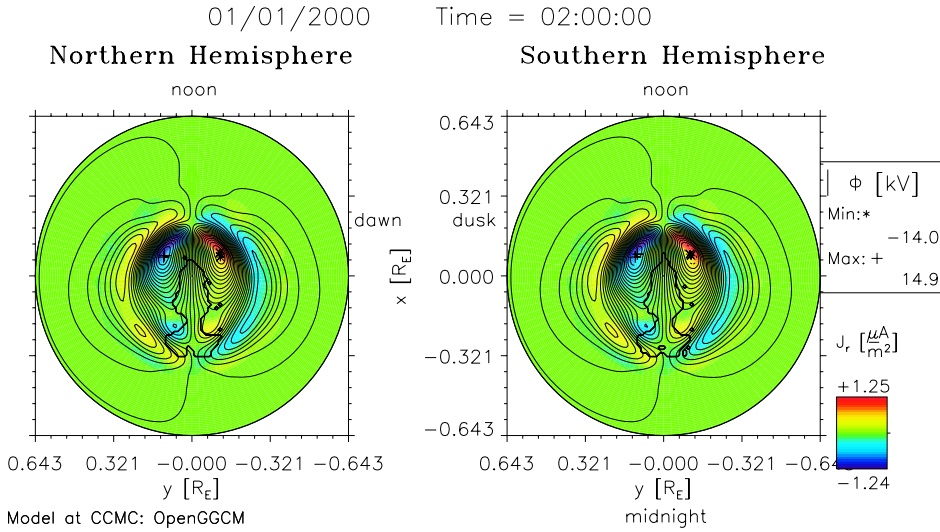
Model at CCMC: LFM

01/01/2000 Time = 02:00:00 UT  $y = 0.00R_E$



Model at CCMC: BATSURS

**IMF  $B_z=5nT$**



Final Comment: we think we understand a lot, but there are still a lot of fundamental unanswered questions, for example:

- To what extent is space weather (like surface weather) predictable, and to what extent is it (like surface weather) inherently unpredictable?
- Why are superthermal particles ubiquitous in space plasmas?
- Most of the solar system is occupied by collisionless plasma. Why are the positive ions, wherever you look, about 5-10 times hotter than the electrons?
- What is role of kinetic-scale processes in determining the large-scale structure of plasmas.?

**Thanks!**